Miki were significantly ($p < 0.05$) lower in cells with these abnormal mitosis/nuclear morphology to compare with those without these abnormalities (Fig. 4G).

Discussion

Here, we identified a microdeletion cluster among JMML patients within 120 kb in 7q21.3 subband. This cluster contains three poorly characterized genes: *Miki* (*LOC253012*), *Samd9*, and *Samd9L*. Since single gene deletion of *Samd9* or *Miki* was proved by two-independent methods (mCGH and qPCR) in patient #1 or #8, respectively, we prefer to consider that three genes, rather than one of them, are candidates for myeloid tumor suppressors on 7q. Three genes are also deleted in adult MDS and AML either as a part of large deletions or single gene loss (Fig. 2C).

Among systems detecting microdeletions, SNP-array hybridization becomes the first choice for primary screening [4]. However, because SNPs tend to cluster within introns and intergenic spaces, SNP-array may not always be the best. For instance, although there are nine SNP probes in this microdeletion cluster in Genome-Wide SNP6.0 system (Affymetrix), no probes can detect *Samd9* gene deletion (Fig. 2A, bottom). In addition, only one probe (A-866741) locates to coding region, casting doubt on the potential of SNP-array to detect small deletions in the critical genes. Application of the short probe-based mCGH to samples containing few copy number abnormalities (such as JMML) would be a good alternative of SNP-array.

In myeloid tumors, −7/7q− has been most implicated in pathogenesis of MDS, which is characterized by myelodysplasia (morphological abnormality in hematopoietic progenitors) [2]. Myelodysplasia includes abnormal nuclear morphologies, such as bi-, tri-, or multi-nucleated cells and abnormal mitoses involving lagging chromosomes, multi-polar mitoses or so-called colchicine-mitosis (chromosome scattering similar to colchicine-treated cells). Despite the fact that these features are routinely observed, underlying molecular mechanisms are largely unknown. Our findings (Fig. 4E–G) raised a possibility that attenuated expression of Miki plays important roles in such abnormal mitosis/nuclear morphology, although detailed mechanisms remained to be established.

Samd9 and Samd9L are related proteins with 60% amino acid identity. Recently, point mutations of Samd9 were reported as a causative gene alterations in Normophosphatemic Familial Tumoral Calcinosis, a rare autosomal recessive disorder in five families of Jewish-Yemenite origin [16,17]. In addition, downregulation of Samd9 was reported to be implicated in aggressive fibromatosis [18], suggesting that Samd9 could be a tumor suppressor. However, Samd9/Samd9L does not show significant homology to any other genes and no biological functions were elucidated. We overexpressed or downregulated Samd9 or Samd9L in various cells and found no prominent phenotype, possibly because functional redundancy of these two proteins. Because there is only *Samd9L* gene in mouse genome [18], *Samd9L*-deficient mice would show unambiguous phenotypes. Indeed, currently we are accumulating phenotypes from *Samd9L*-deficient mice that support our hypothesis that Samd9/Samd9L are myeloid tumor suppressors.

Acknowledgments

We thank Drs. S. Kojima, R. Hanada, M. Kobayashi, K. Koike, and T. Kyo for providing sample. This work was supported by Grants-in-Aid for Scientific Research from the Ministry of Education, Culture, Sports, Science and Technology of Japan.

References

[1] E.J. Freireich, J. Whang, J.H. Tjio, R.H. Levin, G.M. Brittin, I.E. Frei, Refractory anemia, granulocytic hyperplasia of bone marrow, and a missing chromosome in marrow cells. A new clinical syndrome? Clin. Res. 12 (1964) 284.
[2] E.S. Jaffe, N.L. Harris, H. Stein, J.M. Vardiman, Pathology and Genetics of Tumours of Haematopoietic and Lymphoid Tissues, IARC press, Lyon, France, 2001.
[3] R. Todd, B. Bia, E. Johnson, C. Jones, F. Cotter, Molecular characterization of a myelodysplasia-associated chromosome 7 inversion, Br. J. Haematol. 113 (2001) 143–152.
[4] A. Dutt, R. Beroukhim, Single nucleotide polymorphism array analysis of cancer, Curr. Opin. Oncol. 19 (2007) 43–49.
[5] K.K. Mantripragada, I. Tapia-Paez, E. Blennow, P. Nilsson, A. Wedell, J.P. Dumanski, DNA copy-number analysis of the 22q11 deletion-syndrome region using array-CGH with genomic and PCR-based targets, Int. J. Mol. Med. 13 (2004) 273–279.
[6] H.G. Drexler, The Leukemia–Lymphoma Cell Line, Academic Press, London, UK, 2001.
[7] N. Oshimori, M. Ohsugi, T. Yamamoto, The Plk1 target Kizuna stabilizes mitotic centrosomes to ensure spindle bipolarity, Nat. Cell Biol. 8 (2006) 1095–1101.
[8] R. Weksberg, S. Hughes, L. Moldovan, A.S. Bassett, E.W. Chow, J.A. Squire, A method for accurate detection of genomic microdeletions using real-time quantitative PCR, BMC Genomics 6 (2005) 180.
[9] R. Kuribara, H. Honda, H. Matsui, T. Shinjyo, T. Inukai, K. Sugita, S. Nakazawa, H. Hirai, K. Ozawa, T. Inaba, Roles of Bim in apoptosis of normal and Bcr-Abl-expressing hematopoietic progenitors, Mol. Cell. Biol. 24 (2004) 6172–6183.
[10] T. Shinjyo, R. Kuribara, T. Inukai, H. Hosoi, T. Kinoshita, A. Miyajima, P.J. Houghton, A.T. Look, K. Ozawa, T. Inaba, Downregulation of Bim, a proapoptotic relative of Bcl-2. Is a pivotal step in cytokine-initiated survival signaling in murine hematopoietic progenitors, Mol. Cell. Biol. 21 (2001) 854–864.
[11] N. Tokai-Nishizumi, M. Ohsugi, E. Suzuki, T. Yamamoto, The chromokinesin Kid is required for maintenance of proper metaphase spindle size, Mol. Biol. Cell 16 (2005) 5455–5463.
[12] J.H. Griffin, J. Leung, R.J. Bruner, M.A. Caligiuri, R. Briesewitz, Discovery of a fusion kinase in EOL-1 cells and idiopathic hypereosinophilic syndrome, Proc. Natl. Acad. Sci. USA 100 (2003) 7830–7835.
[13] S.W. Horsley, A. Mackay, M. Iravani, K. Fenwick, H. Valgeirsson, T. Dexter, A. Ashworth, L. Kearney, Array CGH of fusion gene-positive leukemia-derived cell lines reveals cryptic regions of genomic gain and loss, Genes Chromosomes Cancer 45 (2006) 554–564.
[14] J. Sebat, B. Lakshmi, J. Troge, J. Alexander, J. Young, P. Lundin, S. Maner, H. Massa, M. Walker, M. Chi, N. Navin, R. Lucito, J. Healy, J. Hicks, K. Ye, A. Reiner, T.C. Gilliam, B. Trask, N. Patterson, A. Zetterberg, M. Wigler, Large-scale copy number polymorphism in the human genome, Science 305 (2004) 525–528.
[15] S. Griffiths-Jones, R.J. Grocock, S. Van Dongen, A. Bateman, A.J. Enright, miRBase: microRNA sequences, targets and gene nomenclature, Nucleic Acids Res. 34 (2006) D140–D144.
[16] O. Topaz, M. Indelman, I. Chefetz, D. Geiger, A. Metzker, Y. Altschuler, M. Choder, D. Bercovich, J. Uitto, R. Bergman, G. Richard, E. Sprecher, A deleterious mutation in SAMD9 causes normophosphatemic familial tumoral calcinosis, Am. J. Hum. Genet. 79 (2006) 759–764.
[17] I. Chefetz, D. Ben Amitai, S. Browning, K. Skorecki, N. Adir, M.G. Thomas, L. Kogleck, O. Topaz, M. Indelman, J. Uitto, G. Richard, N. Bradman, E. Sprecher, Normophosphatemic familial tumoral calcinosis is caused by deleterious mutations in SAMD9, encoding a TNF-alpha responsive protein, J. Invest. Dermatol. 128 (2008) 1423–1429.
[18] C.F. Li, J.R. MacDonald, R.Y. Wei, J. Ray, K. Lau, C. Kandel, R. Koffman, S. Bell, S.W. Scherer, B.A. Alman, Human sterile alpha motif domain 9, a novel gene identified as down-regulated in aggressive fibromatosis, is absent in the mouse, BMC Genomics 8 (2007) 92.

Haploinsufficiency and acquired loss of *Bcl11b* and *H2AX* induces blast crisis of chronic myelogenous leukemia in a transgenic mouse model

Akiko Nagamachi,[1] Norimasa Yamasaki,[2] Kazuko Miyazaki,[2] Hideaki Oda,[3] Masaki Miyazaki,[4] Zen-ichiro Honda,[5] Ryo Kominami,[6] Toshiya Inaba[1] and Hiroaki Honda[2,7]

Departments of [1]Molecular Oncology, [2]Developmental Biology, Research Institute of Radiation Biology and Medicine, Hiroshima University, Hiroshima; [3]Department of Pathology, Tokyo Womens' Medical University, Tokyo; [4]Department of Immunology, Graduate School of Biomedical Sciences, Hiroshima University, Hiroshima; [5]Department of Allergy and Rheumatology, Faculty of Medicine, Graduate School of Medicine, University of Tokyo, Tokyo; [6]Department of Molecular Genetics, Graduate School of Medical and Dental Sciences, Niigata University, Niigata, Japan

(Received February 3, 2009/Revised March 11, 2009/Accepted March 12, 2009/Online publication April 21, 2009)

Chronic myelogenous leukemia (CML) is a hematological malignancy that begins as indolent chronic phase (CP) but inevitably progresses to fatal blast crisis (BC). p210BCR/ABL, a chimeric protein with enhanced kinase activity, initiates CML CP, and additional genetic alterations account for progression to BC, but the precise mechanisms underlying disease evolution are not fully understood. In the present study, we investigated the possible contribution of dysfunction of Bcl11b, a zinc-finger protein required for thymocyte differentiation, and of H2AX, a histone protein involved in DNA repair, to the transition from CML CP to BC. For this purpose, we crossed CML CP-exhibiting *p210BCR/ABL* transgenic (*BA*$^{tg/-}$) mice with *Bcl11b* heterozygous (*Bcl11b*$^{+/-}$) mice and *H2AX* heterozygous (*H2AX*$^{+/-}$) mice. Interestingly, *p210BCR/ABL* transgenic, *Bcl11b* heterozygous (*BA*$^{tg/-}$*Bcl11b*$^{+/-}$) mice and *p210BCR/ABL* transgenic, *H2AX* heterozygous (*BA*$^{tg/-}$*H2AX*$^{+/-}$) mice frequently developed CML BC with T-cell phenotype and died in a short period. In addition, whereas p210BCR/ABL was expressed in all of the leukemic tissues, the expression of Bcl11b and H2AX was undetectable in several tumors, which was attributed to the loss of the residual normal allele or the lack of mRNA expression. These results indicate that Bcl11b and H2AX function as tumor suppressor and that haploinsufficiency and acquired loss of these gene products cooperate with p210BCR/ABL to develop CML BC. (*Cancer Sci* 2009; 100: 1219–1226)

Chronic myelogenous leukemia (CML) is a disorder of hematopoietic stem cells, characterized by excessive and uncontrolled proliferation of differentiated myeloid cells.[1–3] Clinically, CML undergoes two different stages.[1–3] In the initial stage, chronic phase (CP), the leukemic cells retain the ability to differentiate into mature granulocytes and are sensitive to conventional therapies. However, after several years' duration of CP, the disease inevitably accelerates and ultimately progresses to the terminal stage, blast crisis (BC), which exhibits aggressive proliferation of immature blast cells and is resistant to intensive therapies.[1–3]

The cytogenetic hallmark of CML CP is t(9;22)(q34;q11) (known as Philadelphia chromosome, Ph), which generates a *BCR–ABL* fusion gene encoding a 210-kDa chimeric protein (p210BCR/ABL).[1–3] p210BCR/ABL possesses a constitutively active tyrosine kinase activity, which plays an essential role in the initiation of the disease.[1–3] Although Ph is the unique and sole chromosomal abnormality in CP, additional and non-random chromosomal abnormalities are frequently observed in BC, indicating that secondary genetic events account for the disease progression.[1–3]

To understand the pathogenesis of the disease, it is necessary to establish animal models that express *p210BCR/ABL* and recapitulate the clinical course of CML. For this purpose, we generated transgenic mice expressing *p210BCR/ABL* under the control of the mouse *TEC* promoter.[4] The *p210BCR/ABL* transgenic (hereafter, designated as *BA*$^{tg/-}$) mice reproducibly exhibited a myeloproliferative disorder closely resembling human CML CP.[4] In addition, by crossing *BA*$^{tg/-}$ mice with *p53* heterozygous mice and *Dok-1/Dok-2* knockout mice, we showed that the loss of p53 and absence of Dok-1/Dok-2 accelerated the disease and caused CML BC.[5,6] Furthermore, by applying retroviral insertional mutagenesis to *BA*$^{tg/-}$ mice, we demonstrated that overexpression and enhanced kinase activity of p210BCR/ABL and altered expression of Notch1 contribute to CML BC.[7] These results demonstrated that the *BA*$^{tg/-}$ mouse is not only regarded as a model for CML CP, but is also useful for investigating the molecular mechanisms underlying the progression from CP to BC.

Chromosomal and molecular analyses have revealed that several mechanisms are implicated in this process, such as: (i) loss of tumor suppressor; (ii) differentiation arrest; and (iii) chromosomal instability.[3] Indeed, as an example of (i), we demonstrated that loss of p53 cooperates with p210BCR/ABL and induces CML BC.[5,6] In the present report, as candidate genes for (ii) and (iii), we chose *Bcl11b* (also known as *Rit1* and *Ctip2*), encoding a transcription factor required for thymocyte differentiation,[8] and *H2AX*, encoding a histone protein involved in DNA repair,[9] and examined the possible contribution that dysfunction of these gene produces for the disease progression of CML. For this purpose, we crossed *BA*$^{tg/-}$ mice with mice heterozygous for *Bcl11b* (*Bcl11b*$^{+/-}$) or *H2AX* (*H2AX*$^{+/-}$) and generated *BA*$^{tg/-}$*Bcl11b*$^{+/-}$ mice and *BA*$^{tg/-}$*H2AX*$^{+/-}$ mice. Interestingly, both types of double transgenic mouse frequently developed CML BC and died in a short period. The pathological, flow cytometric, molecular, and chromosomal analyses of the diseased mice are described.

Materials and Methods

Mice. *p210BCR/ABL* transgenic, *Bcl11b* heterozygous, and *H2AX* heterozygous mice were generated as described previously.[4,8,10] Crossing and genotyping of the mice were carried out as described previously.[5] All of the mice were kept according to the guidelines of the Institute of Laboratory Animal Science, Hiroshima University.

Pathological analysis. Autopsies were carried out on dead or moribund animals. Peripheral blood smears were stained with Wight-Giemsa. After gross examination, tissues were fixed in

[7]To whom correspondence should be addressed. E-mail: hhonda@hiroshima-u.ac.jp

doi: 10.1111/j.1349-7006.2009.01172.x
© 2009 Japanese Cancer Association

10% neutral buffered formaldehyde and representative slices were stained with hematoxylin–eosin (HE).

Western blot analysis. Proteins were extracted from tissues, separated by SDS-PAGE, transferred to a nitrocellulose membrane, and blotted with appropriate antibodies as described previously.[4,8] The antibodies used in this study were: anti-ABL monoclonal antibody, Ab3 (Oncogene Science, Cambridge, MA, USA); an anti-Bcl11b polyclonal antibody;[8] and an antihistone H2AX antibody (Millipore, Bedford, MA, USA). Positive signals were detected with the enhanced chemiluminescence system.

Southern blot analysis and genomic PCR. For Southern blotting, DNA was digested with restriction enzymes, separated in an agarose gel, blotted to a nylon membrane, and hybridized with a ^{32}P-dCTP-labeled *TCRβ* probe. Genomic PCR was carried out using the following primers as described previously:[11] P1 (5′-TGCAGCTTTCCGGGCGATGCCA-3′), P2 (5′-ACTTTCCCAG-AACCCCACGC-3′), and P3 (5′-CCTGCTTGCCGAATATCAT-GGTGG-3′) for *Bcl11b*; and P1 (5′-TCACATTGTTTCCTTCG-GTGTCAC-3′), P2 (5′-AAGTGTTGTGATTGGGAAGCGTAG-3′), P3 (5′-AGATCCCGTTGACTGAACACAGG-3′), P4 (5′-TTCAG-GTTTTGTTGTCGCGCCGTAG-3′), and P5 (5′-TCAGCTCTTT-CTGTGAGGGAGGTGG-3′) for *H2AX*.

Northern blot analysis and RT-PCR. Total RNA was extracted using TRIzol (Invitrogen, Carlsbad, CA, USA), separated in 1.2% formaldehyde gel, blotted to a nylon membrane, and hybridized with a ^{32}P-dCTP-labeled *H2AX* probe. RT-PCR was carried out using the following primers as described previously:[11] 5′-CGAGCTCA-GGAAAGTGTCCGAG-3′ and 5′-GGAAATTCATGAGCGGG-GACTG-3′ for *Bcl11b*; 5′-CCTTCTGGAAGACTTGGCCTTC-3′ and 5′-GAGGAAGATGTGCCTGTTACC-3′ for *H2AX*; and 5′-TTCAACACCCCAGCCATGTA-3′ and 5′-CTCAGGAGGAG-CAATGATCT-3′ for *β-actin*.

Flow cytometric analysis. Cells were stained with FITC- or phycoerythrin (PE)-conjugated anti-Thy-1.2, anti-B220, anti-Mac1, and anti-Gr1 monoclonal antibodies (Pharmingen, San Diego, CA, USA), as described previously.[5]

Chromosomal analysis. Chromosomes were prepared by means of standard culture procedures for tumor cells and treated with trypsin-Giemsa as described previously.[12]

Patient samples and normal bone marrow cells. Patient samples were taken after obtaining informed consent and approval from the institutional review board at Hiroshima University.[13] Diagnosis of CML CP or CML BC (myeloid or B-lymphoid lineage) was carried out based on morphological, cytogenetic, and immunophenotypic analyses. Normal bone marrow cells were obtained from a healthy volunteer.

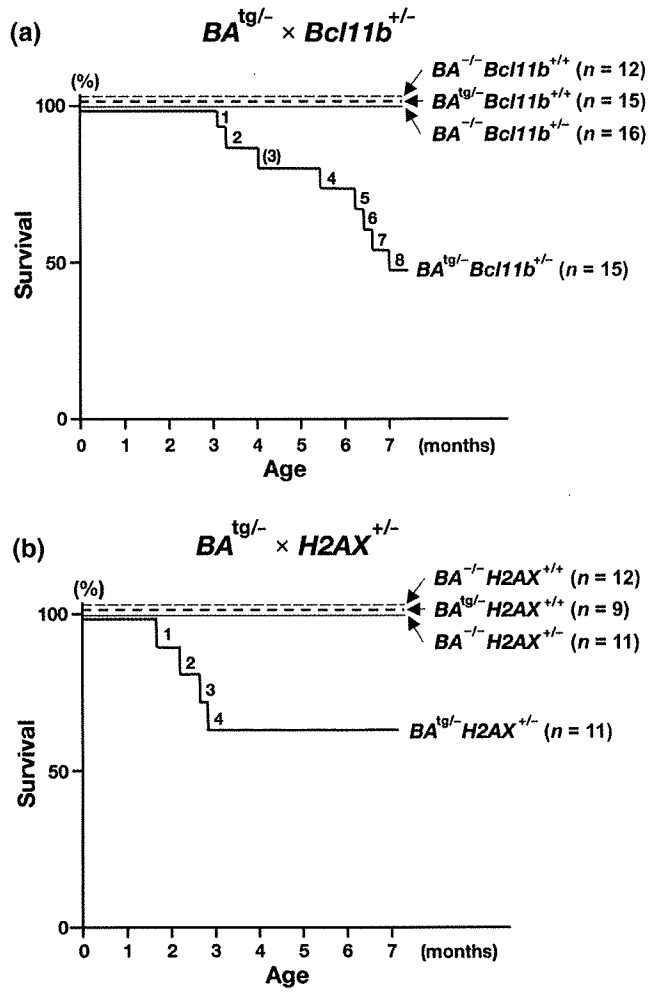

Fig. 1. Survival curves of mice generated by (a) $BA^{tg/-} \times Bcl11b^{+/-}$ and (b) $BA^{tg/-} \times H2AX^{+/-}$. The survival curves of $BA^{-/-}Bcl11b^{+/+}$ and $BA^{-/-}HX2A^{+/+}$, $BA^{tg/-}Bcl11b^{+/+}$ and $BA^{tg/-}H2AX^{+/+}$, $BA^{-/-}Bcl11b^{+/-}$ and $BA^{-/-}H2AX^{+/-}$, and $BA^{tg/-}Bcl11b^{+/-}$ and $BA^{tg/-}H2AX^{+/-}$ mice are shown as thin dotted, thick dotted, thin continuous, and thick continuous lines respectively. In the $BA^{tg/-} \times Bcl11b^{+/-}$ group, 8 of 15 $BA^{tg/-}Bcl11b^{+/-}$ mice died within 7 months of age and in the $BA^{tg/-} \times H2AX^{+/-}$ group, 4 of 11 $BA^{tg/-}H2AXb^{+/-}$ died within 3 months of age. The number of an unanalyzable $BA^{tg/-}Bcl11b^{+/-}$ mouse due to death (no. 3) is shown in parentheses.

Results

***$BA^{tg/-}Bcl11b^{+/-}$* and *$BA^{tg/-}H2AX^{+/-}$* mice developed acute leukemia and died in a short period.** To investigate the contribution of haploinsufficiency of *Bcl11b* and *H2AX* to the disease progression of CML, we crossed CML-exhibiting $BA^{tg/-}$ mice with $Bcl11b^{+/-}$ mice and $H2AX^{+/-}$ mice. Mice with four different genotypes were generated by each crossing: $BA^{tg/-} \times Bcl11b^{+/-}$ created $BA^{-/-}Bcl11b^{+/+}$ (wild type), $BA^{tg/-}Bcl11b^{+/+}$ (*p210BCR/ABL* transgenic), $BA^{-/-}Bcl11b^{+/-}$ (*Bcl11b* heterozygous), and $BA^{tg/-}Bcl11b^{+/-}$ (*p210BCR/ABL* transgenic, *Bcl11b* heterozygous); and $BA^{tg/-} \times H2AX^{+/-}$ produced $BA^{-/-}H2AX^{+/+}$ (wild type), $BA^{tg/-}H2AX^{+/+}$ (*p210BCR/ABL* transgenic), $BA^{-/-}H2AX^{+/-}$ (*H2AX* heterozygous), and $BA^{tg/-}H2AX^{+/-}$ (*p210BCR/ABL* transgenic, *H2AX* heterozygous). Mice with these genotypes were normally born approximately at the expected Mendelian ratio (see the mouse number shown in parentheses in Fig. 1), indicating that the crossing did not affect the embryonic development of the mice.

All of the mice were observed continuously and peripheral blood parameters were counted routinely. The genotype-based survival curves of the mice in each crossing are shown in Figure 1. During a 7-month observation period, in the $BA^{tg/-} \times Bcl11b^{+/-}$ group, 8 of 15 $BA^{tg/-}Bcl11b^{+/-}$ died of acute leukemia, in contrast $BA^{-/-}Bcl11b^{+/+}$, $BA^{tg/-}Bcl11b^{+/+}$, and $BA^{-/-}Bcl11b^{+/-}$ littermates did not show any disorders (Fig. 1a). As for the $BA^{tg/-} \times H2AX^{+/-}$ group (lower panel), 4 of 11 $BA^{tg/-}H2AX^{+/-}$ mice exhibited proliferation of blast cells and died within 3 months of birth, whereas no disease was observed in $BA^{-/-}H2AX^{+/+}$, $BA^{tg/-}H2AX^{+/+}$, and $BA^{-/-}H2AX^{+/-}$ littermates (Fig. 1b).

The representative results of pathological analysis of $BA^{tg/-}Bcl11b^{+/-}$ and $BA^{tg/-}H2AX^{+/-}$ leukemic mice are shown in Figure 2. Macroscopically, both leukemic mice exhibited marked thymic enlargement with splenomegaly, which were occasionally associated with lymph node swelling or pleural effusion (data not shown). The peripheral blood smears exhibited proliferation of blast cells morphologically resembling lymphoblasts (upper panels of Fig. 2). Tissue sections showed that the blast cells caused destruction of the basic structure of the thymus (second panels of Fig. 2) and infiltrated in non-hematopoietic tissues, such as liver (third panels of Fig. 2). In contrast, the bone marrow

doi: 10.1111/j.1349-7006.2009.01172.x
© 2009 Japanese Cancer Association

Table 1. Characteristics of *p210BCR/ABL*$^{tg/-}$ *Bcl11b*$^{+/-}$ leukemic mice

Mouse no.	Age at disease (months)	PB parameters			Macroscopic tumor sites	*TCRβ* status	p210BCR/ABL expression	Bcl11b expression	*Bcl11b* status
		WBC ($\times 10^3/\mu L$)	Hb (g/dL)	Plt ($\times 10^4/\mu L$)					
1	3.1	35.0	12.5	65.6	Thy, Spl	G/R	+	+	G/T
2	3.3	5.0	10.5	64.8	Thy, Spl	G/loss	+	+	G/T
3	4.0†	ND	ND	ND	Thy	ND	ND	ND	ND
4	5.3	2.3	7.1	44.2	Thy	G/loss	+	+	G/T
5	6.0	12.0	12.3	35.5	Thy, PE	G/loss	+	–	T/loss
6	6.1	6.6	13.9	53.5	Thy	G/R	+	–	T/loss
7	6.4	14.6	15.5	47.1	Thy, Spl	G/R	+	+	G/T
8	6.9	1.5	14.1	74.9	Thy, PE	G/R	+	–	T/loss

†Found dead. G, germline; Hb, hemoglobin; ND, not done; PB, peripheral blood; PE, pleural effusion; Plt, platelet; R, rearranged; Spl, spleen; T, targeted; Thy, thymus; WBC, white blood cell.

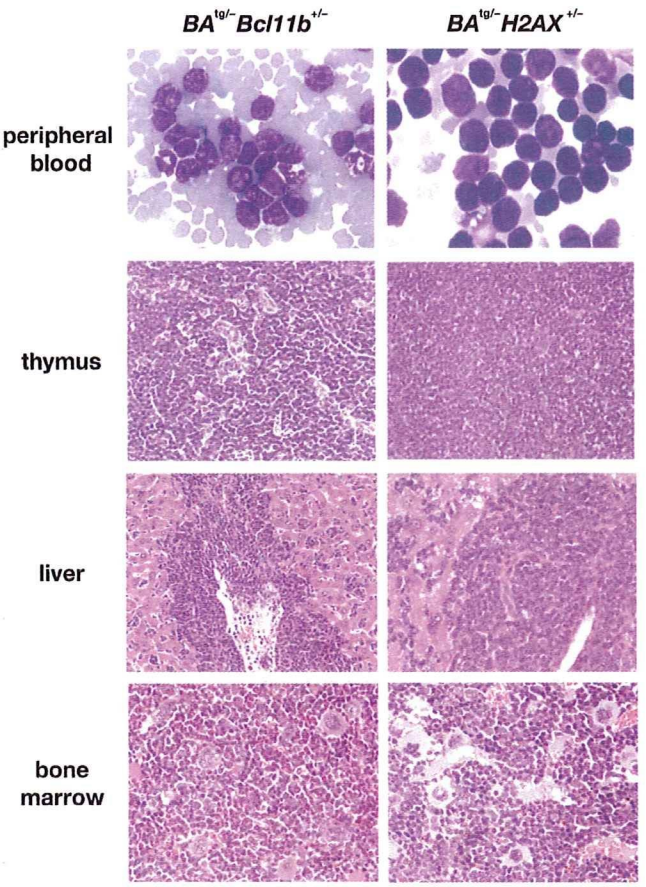

Fig. 2. Representative results of pathological analysis of *BA*$^{tg/-}$*Bcl11b*$^{+/-}$ (left panels) and *BA*$^{tg/-}$*H2AX*$^{+/-}$ (right panels) leukemic mice. Wight-Giemsa-stained peripheral blood smears and HE-stained tissue slices are shown. In both leukemic mice, blast cells proliferated in the peripheral blood (upper panels), caused destruction of the basal structure of the thymus (second panels), and infiltrated around the vessel and in the sinusoids in the liver (third panels). In contrast, bone marrow exhibited myeloid cell hyperplasia with differentiation and proliferation of megakaryocytes (bottom panels).

showed a predominance of myeloid cells with differentiation and proliferation of megakaryocytes (bottom panels of Fig. 2). These results demonstrated that haploinsufficiency of *Bcl11b* and *H2AX* cooperated with *p210BCR/ABL*, transformed *p210BCR/ABL*-expressing hematopoietic cells, and caused CML BC. The characteristics of *BA*$^{tg/-}$*Bcl11b*$^{+/-}$ and *BA*$^{tg/-}$*H2AX*$^{+/-}$ leukemic mice are summarized in Table 1 and Table 2, respectively.

Leukemias that developed in *BA*$^{tg/-}$*Bcl11b*$^{+/-}$ and *BA*$^{tg/-}$*H2AX*$^{+/-}$ mice were of T-cell lineage and were mostly clonal in origin. To determine the cell lineage and clonality of the leukemias that developed in *BA*$^{tg/-}$*Bcl11b*$^{+/-}$ and *BA*$^{tg/-}$*H2AX*$^{+/-}$ mice, blast cells were subjected to flow cytometric and Southern blot analyses.

The representative results of flow cytometric analysis of *BA*$^{tg/-}$*Bcl11b*$^{+/-}$ and *BA*$^{tg/-}$*H2AX*$^{+/-}$ leukemic cells are shown in Figure 3(a). In both types of mice, leukemic cells were highly positive for Thy1.2, the antigen specific for T lymphocytes, but were negative for CD19, Gr1, and Mac1, the markers for B lymphocytes, granulocytes, and macrophages respectively.

The clonality of the leukemic cells was examined by gene rearrangement analysis. DNA extracted from a control thymus and tumor tissues of *BA*$^{tg/-}$*Bcl11b*$^{+/-}$ and *BA*$^{tg/-}$*H2AX*$^{+/-}$ leukemic mice were digested with a restriction enzyme and blotted with the T-cell receptor β (*TCR-β*) gene. As shown in Figure 3(b), more than half of the samples (no. 1 and no. 6–8 in *BA*$^{tg/-}$*Bcl11b*$^{+/-}$ and no. 1 and 2 in *BA*$^{tg/-}$*H2AX*$^{+/-}$) showed rearranged bands, and in the remaining samples (no. 2, 4, and 5 in *BA*$^{tg/-}$*Bcl11b*$^{+/-}$ and no. 3 and 4 in *BA*$^{tg/-}$*H2AX*$^{+/-}$), loss of the upper germline band was observed (the positions of germline bands are indicated by arrows and shown as 'G'). These results demonstrated that the blast cells of *BA*$^{tg/-}$*Bcl11b*$^{+/-}$ and *BA*$^{tg/-}$*H2AX*$^{+/-}$ leukemic mice were committed to the T-cell lineage and most of the tumors were clonal in origin.

Frequent and acquired loss of Bcl11b and H2AX protein expression in the tumor tissues of *BA*$^{tg/-}$*Bcl11b*$^{+/-}$ and *BA*$^{tg/-}$*H2AX*$^{+/-}$ leukemic mice. We then investigated protein expression in the tumor tissues of *BA*$^{tg/-}$*Bcl11b*$^{+/-}$ and *BA*$^{tg/-}$*H2AX*$^{+/-}$ leukemic mice. Proteins extracted from a control thymus and tumor tissues of *BA*$^{tg/-}$*Bcl11b*$^{+/-}$ and *BA*$^{tg/-}$*H2AX*$^{+/-}$ leukemic mice were blotted with antibodies against c-ABL, Bcl11b, and H2AX.

The results of p210BCR/ABL expression in these tumors are shown in the upper panels of Figure 4(a,b). As shown in both panels, the 210-kDa band was detected in all of the tumor samples, indicating that the blast cells originated from *p210BCR/ABL*-expressing hematopoietic precursors. We next examined the expression of Bcl11b and H2AX proteins in *BA*$^{tg/-}$*Bcl11b*$^{+/-}$ and *BA*$^{tg/-}$*H2AX*$^{+/-}$ leukemic samples respectively. Interestingly, in the anti-Bcl11b western blot, the expression of Bcl11b was found to be lost in three of seven samples (no. 5, 6, and 8, middle panel of Fig. 4a). In addition, in the anti-H2AX blot, the expression of H2AX was undetectable in two of four samples (no. 2 and 3, middle panel of Fig. 4b). These results indicated that the protein expression of Bcl11b and H2AX was lost in several samples of *BA*$^{tg/-}$*Bcl11b*$^{+/-}$ and *BA*$^{tg/-}$*H2AX*$^{+/-}$ leukemic mice.

To investigate the molecular mechanism underlying the loss of Bcl11b and H2AX expression, DNA extracted from tumor

© 2009 Japanese Cancer Association

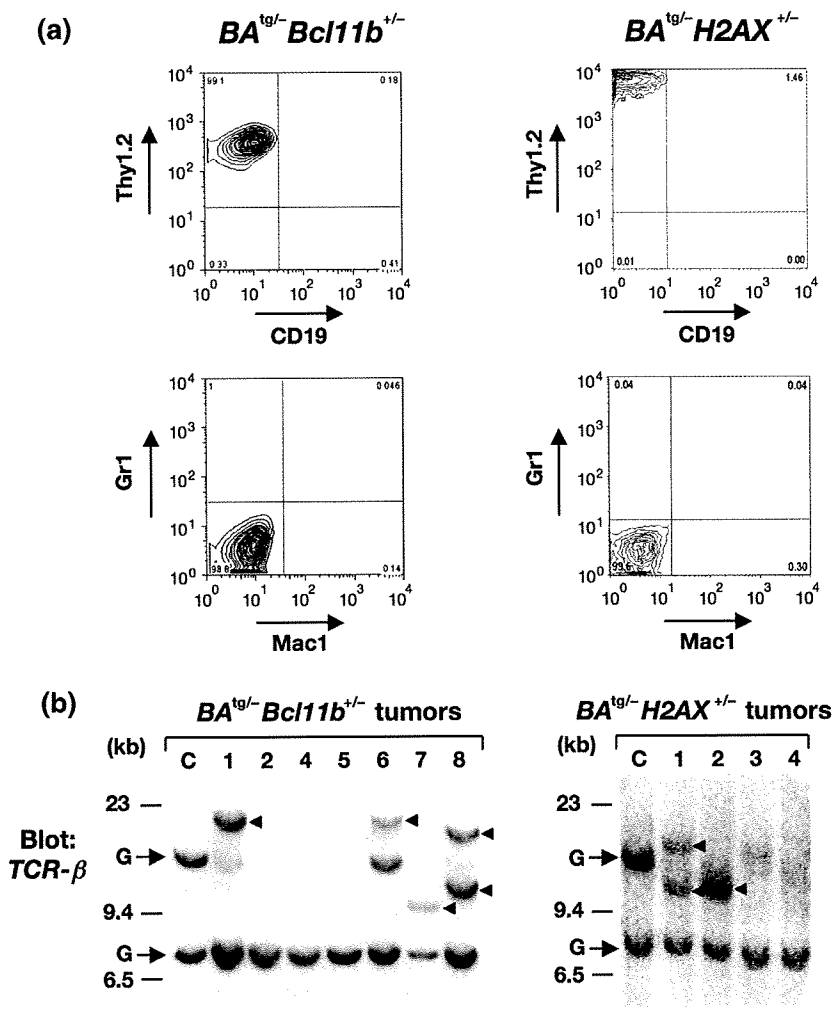

Fig. 3. Results of flow cytometric and Southern blot analyses of *BA*$^{tg/-}$*Bcl11b*$^{+/-}$ and *BA*$^{tg/-}$*H2AX*$^{+/-}$ leukemic mice. (a) Representative results of flow cytometry of leukemic cells that developed in *BA*$^{tg/-}$*Bcl11b*$^{+/-}$ (left panel) and *BA*$^{tg/-}$*H2AX*$^{+/-}$ (right panel) mice. In both samples, blast cells were positive for Thy1.2 but negative for CD19, Gr1, and Mac1, indicating that they were of T-cell phenotype. (b) Results of gene rearrangement analysis in tumors that developed in *BA*$^{tg/-}$*Bcl11b*$^{+/-}$ (left panel) and *BA*$^{tg/-}$*H2AX*$^{+/-}$ (right panel) mice. (c) DNA extracted from control thymus and thymomas that developed in *BA*$^{tg/-}$*Bcl11b*$^{+/-}$ (left panel) and *BA*$^{tg/-}$*H2AX*$^{+/-}$ (right panel) mice were digested with *Bam*HI and blotted with *TCR-β* probe. Germline and rearranged bands are indicated by arrows and arrowheads respectively. Molecular markers are shown on the left.

Table 2. Characteristics of p210BCR/ABL$^{tg/-}$ H2AX$^{+/-}$ leukemic mice

Mouse no.	Age at disease (months)	PB parameters			Macroscopic tumor sites	*TCRβ* status	p210BCR/ABL expression	H2AX expression	H2AX status
		WBC (× 10^3/μL)	Hb (g/dL)	Plt (× 10^4/μL)					
1	1.8	15.3	16.1	56.4	Thy, Spl	G/R	+	+	G/T
2	2.2	160.8	10.4	53.4	Thy, Spl, LN	G/R	+	–	G/T
3	2.5	128.4	12.0	90.9	Thy, Spl, LN	G/loss	+	–	G/T
4	2.8	84.7	12.4	36.0	Thy, Spl, LN	G/loss	+	+	G/T

G, germline; LN, lymph node; R, rearranged; Spl, spleen; T, targeted; Thy, thymus.

tissues was subjected to genomic PCR that distinguished the PCR product of the wild-type allele from that of the knockout allele (upper panels of Fig. 4c,d). The results showed that the wild-type *Bcl11b* allele-derived band was not amplified in the three samples without Bcl11b expression (no. 5, 6, and 8, lower panel of Fig. 4c), indicating that the absence of Bcl11b protein was attributed to the loss of the residual wild-type *Bcl11b* allele. In contrast, the PCR product from the wild-type *H2AX* allele was retained in the two samples lacking H2AX expression (no. 2 and 3 in the lower panel of Fig. 4d). Because the PCR primer set detecting the wild-type allele (P1 + P2) did not amplify the coding region of the *H2AX* gene (upper panel of Fig. 4d), we designed another primer set encompassing the *H2AX* exon. As *H2AX* is a single-exon gene,[10] this primer set (shown as P4 and P5 in the upper panel of Fig. 4d) amplified a part of the promoter and the whole coding region. The results showed that a PCR product of expected size was detected in all of the *BA*$^{tg/-}$*H2AX*$^{+/-}$ tumors (lower panel of Fig. 4d). To examine the possibility that subtle deletion and/or base substitution had occurred in this region, we sequenced the whole PCR product but could not detect any mutation (data not shown). In addition, Southern blotting using a 5′ external probe for the *H2AX* gene[10] did not show any gross rearrangement (data not shown). These results indicated that the structure of the *H2AX* gene was largely unaffected. We next examined H2AX mRNA expression in the *BA*$^{tg/-}$*H2AX*$^{+/-}$ tumors by northern blotting. Interestingly, as shown

doi: 10.1111/j.1349-7006.2009.01172.x
© 2009 Japanese Cancer Association

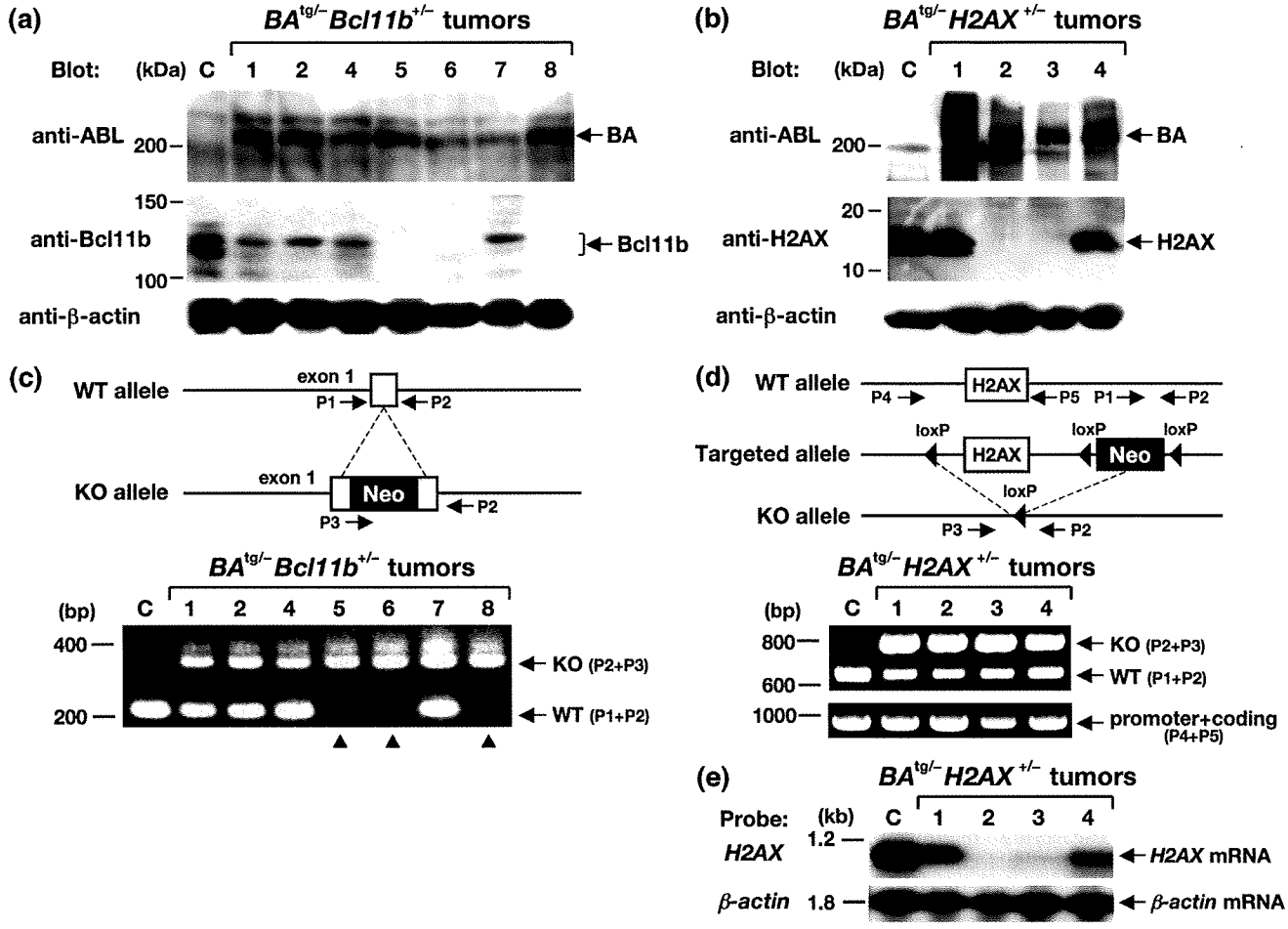

Fig. 4. Gene expression and PCR analyses of the tumors that developed in *BA*$^{tg/-}$*Bcl11b*$^{+/-}$ (left panels) and *BA*$^{tg/-}$*H2AX*$^{+/-}$ (right panels) mice. (a,b) Western blot analysis for the expression of p210BCR/ABL, Bcl11b, and H2AX proteins. Proteins extracted from a control (C) thymus and tumor tissues of *BA*$^{tg/-}$*Bcl11b*$^{+/-}$ (no. 1, 2, and 4–8) and *BA*$^{tg/-}$*H2AX*$^{+/-}$ mice (no. 1–4) were blotted with an anti-ABL antibody (upper panels) and anti-Bcl11b or anti-H2AX antibody (middle panels). The positions of p210BCR/ABL (BA), Bcl11b, and H2AX proteins are indicated by arrows. An anti-β-actin blot was carried out as an internal control (bottom panels). Protein markers are shown on the left. (c,d) Schematic illustrations of wild-type and targeted alleles for *Bcl11b* and *H2AX* genes (upper panels) and the resultant genomic PCR products (lower panels). DNA extracted from a control (C) thymus and tumor tissues of *BA*$^{tg/-}$*Bcl11b*$^{+/-}$ (no. 1, 2 and 4–8) and *BA*$^{tg/-}$*H2AX*$^{+/-}$ mice (no. 1–4) were amplified with sets of primers (P1 and P2 for wild-type [WT] alleles, P2 and P3 for knockout [KO] alleles, and P4 and P5 for a part of the promoter and the whole coding region of *H2AX*). The positions of primers are shown in the upper panels and WT- and KO-derived PCR products are indicated by arrows in the lower panels. Molecular markers are shown on the left. Samples without *Bcl11b* expression are indicated by arrowheads. *Neo*, neomycin resistance gene. (e) Expression of *H2AX* mRNA in *BA*$^{tg/-}$*H2AX*$^{+/-}$ tumors. RNA extracted from a control thymus (C) and tumor tissues of *BA*$^{tg/-}$*H2AX*$^{+/-}$ mice (no. 1–4) were hybridized with *H2AX* cDNA probe. *β-Actin* hybridization was carried out as an internal control. Molecular markers are shown on the left.

in Figure 4(e), no H2AX mRNA was detected in tumors lacking H2AX protein expression (no. 2 and 3). These results indicated that the absence of H2AX protein was not due to deletion or mutation in the *H2AX* gene but to a lack of mRNA expression.

Chromosomal abnormalities in the leukemic cells developed in *BA*$^{tg/-}$*H2AX*$^{+/-}$ mice. We finally examined the chromosomal status of the leukemic cells developed in *BA*$^{tg/-}$*H2AX*$^{+/-}$ mice, as previous reports demonstrated that haploinsufficiency and absence of H2AX led to increased incidence of chromosomal abnormalities.[14,15] In the four tumors that arose from *BA*$^{tg/-}$*H2AX*$^{+/-}$ mice, although two samples showed a normal karyotype (no. 1 and 4, data not shown), the other two samples (no. 2 and 3) that did not express H2AX protein (Fig. 4b) exhibited chromosomal aberrations. As shown in the left panel of Figure 5, sample no. 2 contained an additional chromosome (indicated by an arrowhead). In addition, as shown in the right panel of Figure 5, sample no. 3 exhibited deletions in the long arm of chromosome 6 and in the short arm of chromosome 13, and a breakage in chromosome 11 (indicated by arrows). These results suggested the possibility that the acquired loss of H2AX induced chromosomal instability and resulted in the chromosomal abnormalities observed in samples no. 2 and 3.

Discussion

Chronic myelogenous leukemia presents a paradigm for cancers that evolve through accumulation of genetic alterations. Generation of p210BCR/ABL initiates CML CP and additional genetic events progress the disease and develop CML BC.[1–3] Although chromosomal and molecular analyses revealed that various mechanisms are involved in the transition from CP to BC,[1–3] genes responsible for the evolution to BC have not fully been identified.

To elucidate the mechanisms underlying the disease evolution of CML, we have developed an *in vivo* model for CML in which expression of *p210BCR/ABL* induces CML CP, and additional

© 2009 Japanese Cancer Association

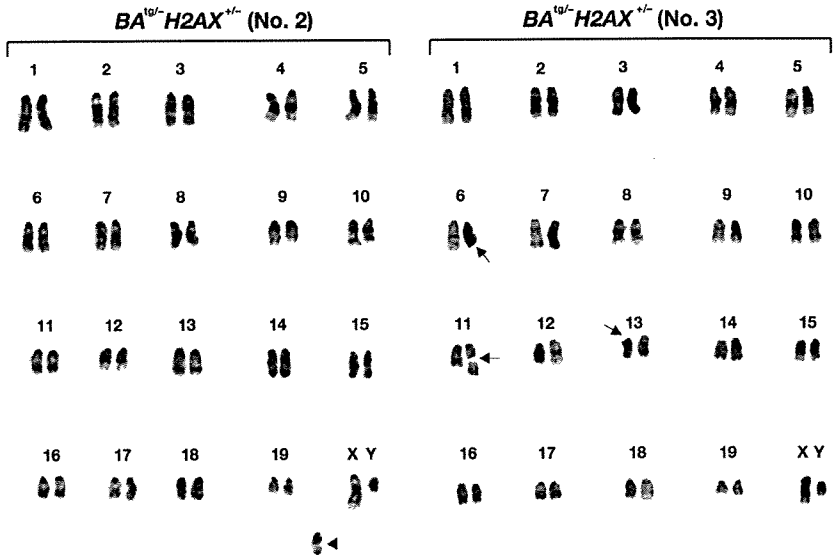

Fig. 5. Chromosomal abnormalities observed in two tumors (no. 2 and 3) that developed in $BA^{tg/-}H2AX^{+/-}$ mice. The additional chromosome in tumor no. 2 is indicated by an arrowhead, and deletion and breakage of the chromosomes in tumor no. 3 are indicated by arrows.

genetic alterations cooperate with *p210BCR/ABL* to progress the disease to CML BC.[4–7] Using this as a model system, we examined the possible contribution of haploisufficiency of *Bcl11b* and *H2AX* to CML BC, by crossing *p210BCR/ABL* transgenic mice ($BA^{tg/-}$) with *Bcl11b* heterozygotes ($Bcl11b^{+/-}$) and *H2AX* heterozygotes ($H2AX^{+/-}$).

Bcl11b encodes a zinc finger protein involved in thymocyte development and differentiation.[8] *Bcl11b* was originally identified as a gene homologous to *Bcl11a*, that was cloned from t(2;14)(p13;q32.3)-carrying malignant lymphomas,[16] and subsequently shown to be frequently deleted or mutated in radiation-induced thymoma in mice.[17] Conditional knockout analysis showed that acquired ablation of *Bcl11b* in thymocytes resulted in impaired positive selection, altered T-cell receptor signaling, and reduced survival.[18] In addition, a recent study revealed that *Bcl11b* is involved in human leukemia carrying inv(14)(q11.2q32.31), which resulted in generation of the *Bcl11b–TRDC* fusion transcript.[19] On the other hand, H2AX is a member of the histone H2A family and a constituent of the nucleosome, the basic subunit of chromatin.[9,20,21] In response to the DNA double-strand break, H2AX rapidly becomes phosphorylated on the serine residue located at the C-terminus to form γH2AX at the DNA double-strand break sites.[9,20,21] This event creates a focus in the nucleus, where DNA repair and chromatin remodeling proteins are recruited.[9,20,21] In human hematopoietic malignancies, a single nucleotide polymorphism upstream of the *H2AX* gene was found to be tightly associated with susceptibility to non-Hodgkin lymphoma.[22] These results indicated that *Bcl11b* and *H2AX* are functionally implicated in cell differentiation and chromosomal stability, respectively, and are involved in subsets of hematopoietic malignancies.

We found that 8 of 15 $BA^{tg/-}Bcl11b^{+/-}$ mice and 4 of 11 $BA^{tg/-}H2AX^{+/-}$ mice developed acute leukemia and died in a short period (Fig. 1). These results indicated that haploinsufficiency of *Bcl11b* and *H2AX* conferred a growth advantage to *p210BCR/ABL*-expressing hematopoietic cells and consequently induced acute leukemia. The blast cells were highly malignant, as evidenced by massive proliferation in the peripheral blood, destruction of the basic structure of the thymus, and marked infiltration in non-hematopoietic tissues (upper 3 panels of Fig. 2). Surface marker analysis showed that the leukemic cells were of T-cell phenotype and Southern blot analysis demonstrated that most of the tumors were clonal in origin (Fig. 3). As the bone marrow showed the typical picture of CML CP (bottom panels of Fig. 2), the leukemias that developed in $BA^{tg/-}Bcl11b^{+/-}$ and $BA^{tg/-}H2AX^{+/-}$ mice were considered to be CML T-cell BC rather than *de novo* T-cell malignancy.

Interestingly, protein analysis revealed that the expression of Bcl11b and H2AX was lost in several tumors that developed in the $BA^{tg/-}Bcl11b^{+/-}$ and $BA^{tg/-}H2AX^{+/-}$ mice (Fig. 4a,b, middle panels). These results strongly suggested that the expression of p210BCR/ABL rendered genetic instability in the hematopoietic cells and consequently lost the normal residual allele of *Bcl11b* and *H2AX*, as reported in our previous study.[5] Indeed, in $BA^{tg/-}Bcl11b^{+/-}$ tumors, genomic PCR analysis revealed that the wild-type *Bcl11b*-derived band was not amplified in tumors lacking Bcl11b expression (no. 5, 6, and 8 in the lower panel of Fig. 4c), indicating that loss of the normal *Bcl11b* allele was responsible for the lack of the protein product. In contrast, the tumor tissues with no H2AX expression in $BA^{tg/-}H2AX^{+/-}$ mice retained the normal *H2AX* allele, including the 3′ region, a part of the promoter region, and the whole coding region (no. 2 and 3 in the lower panels of Fig. 4d). Instead, we found that no H2AX mRNA was expressed in tumors lacking H2AX protein (no. 2 and 3 in the upper panel of Fig. 4e), which indicated that the absence of H2AX protein was due to the lack of H2AX mRNA expression. Although the mechanism underlying loss of the *H2AX* message in these tumors remains unclear, one possibility is that *p210BCR/ABL*-induced genetic alterations might have occurred in the other regions regulating *H2AX* transcription, such as the enhancer, which led to the loss of mRNA expression. Alternatively, p210BCR/ABL might have impaired the transcriptional machinery for H2AX mRNA in these tumors by an unknown mechanism. Taken together, our findings demonstrated that p210BCR/ABL induces loss of protein expression through several different mechanisms, including genomic instability and transcriptional inhibition.

It is to be noted that four $BA^{tg/-}Bcl11b^{+/-}$ and two $BA^{tg/-}H2AX^{+/-}$ leukemic mice retained Bcl11b and H2AX protein expression (no. 1, 2, 4, and 7 in the middle panel of Fig. 4a and no. 1 and 4 in the middle panel of Fig. 4b). Thus, the mechanism of how haploinsufficiency of these genes caused disease evolution is to be clarified. Although no obvious phenotypic abnormalities were found in $Bcl11b^{+/-}$ or $H2AX^{+/-}$ mice, previous studies demonstrated that both types of heterozygotes exhibit enhanced susceptibility to hematological malignancies on $p53^{+/-}$ and $p53^{-/-}$ backgrounds.[14,15,23] These results indicated that both genes function as a dosage-dependent tumor suppressor and their

doi: 10.1111/j.1349-7006.2009.01172.x
© 2009 Japanese Cancer Association

haploinsufficiency predisposes to cancer development in certain genetic backgrounds. Thus, it is possible that haploinsufficiency of *Bcl11b* and *H2AX* exerted its oncogenic potential in cooperation with *p210BCR/ABL*, conferred a growth advantage to *p210BCR/ABL*-expressing hematopoietic cells, and consequently developed CML BC. An alternative possibility is that because p210BCR/ABL is known to promote genetic instability,[3,5] altered expression of unknown genes synergized with haploinsufficient *Bcl11b* or *H2AX* in *p210BCR/ABL*-expressing hematopoietic cells, accelerated progression of CML, and eventually caused CML BC.

We finally examined the possible chromosomal abnormalities in the leukemic cells of $BA^{tg/-}H2AX^{+/-}$ mice, as previous reports demonstrated that haploinsufficiency or deficiency of *H2AX* induced various chromosomal aberrations, especially on a $p53^{-/-}$ genetic background.[14,15] The results showed that two of four tumors exhibited chromosomal abnormalities, which were the presence of an additional chromosome, deletion in part of the long and short arms, and breakage in the body of several chromosomes (Fig. 5). Interestingly, $BA^{tg/-}H2AX^{+/-}$ mice with these chromosomal abnormalities exhibited very high white blood cell (WBC) counts ($>1 \times 10^5/\mu L$, see the right top panel of Fig. 2 and Table 2), suggesting that these events conferred a marked proliferative ability to *p210BCR/ABL*-expressing hematopoietic cells and exhibited a very aggressive phenotype. We also examined the possible contribution of dysfunction of genes involved in error-prone non-homologous end joining, such as *DNA ligase IV* and *XRCC4*, by crossing $BA^{tg/-}$ with *DNA ligase IV* heterozygous mice and *XRCC4* heterozygous mice. However, we did not observe disease acceleration or CML BC in $BA^{tg/-}$*DNA ligase* $IV^{+/-}$ or $BA^{tg/-}XRCC4^{+/-}$ double transgenic mice (data not shown), suggesting the possibility that among DNA repair-associated genes, *H2AX* might play a unique role in the disease evolution of CML.

The CML BC observed in $BA^{tg/-}Bcl11b^{+/-}$ and $BA^{tg/-}H2AX^{+/-}$ mice were of T-cell phenotype. Although T-cell BC is frequently observed in mouse models for CML,[5,24] it is rarely detected in human clinical samples. The reason for this discrepancy is not clear but one possibility is that human CML originates from the acquisition of *p210BCR/ABL*-transformed hematopoietic stem cells and the T-cell lineage is rarely involved probably due to its prolonged life span, whereas every cell in transgenic (or knockout) mice inherently contains (or lacks) the target gene and T cells might be more susceptible to the target gene-induced oncogenic transformation than other types of hematopoietic cells.

It is intriguing to examine whether acquired expressional loss of *Bcl11b* and *H2AX* contributes to human CML BC. We examined *Bcl11b* and *H2AX* expression in several CML BC samples by RT-PCR but did not detect the absence of mRNA expression in either gene (Supporting Information Fig. S1), probably due to the limited number of samples available and a lack of T-cell crisis cases. Thus, an expanded study is required to clarify the clinical significance of dysfunction of these genes in the development of CML BC.

In the present report, we demonstrated that haploinsufficiency and acquired loss of protein expression of *Bcl11b* and *H2AX* cooperate with *p210BCR/ABL* and induce CML BC. Our findings demonstrated that altered expression of genes involved in cell differentiation or chromosomal integrity contributes to the development of CML BC, which provides insights into the molecular mechanisms underlying the disease evolution of CML.

Acknowledgments

This work was supported by a Grant-in-Aid from the Ministry of Education, Science, and Culture of Japan, a Grant-in-Aid for Cancer Research from the Ministry of Health, Labour, and Welfare of Japan (13-2), Research Grant of the Princess Takamatsu Cancer Research Fund, Astellas Research Foundation, YASUDA Medical Research Foundation, a Grant-in-Aid of The Japan Medical Association, and Japan Leukaemia Research Fund.

References

1 Calabretta B, Perrotti D. The biology of CML blast crisis. *Blood* 2004; **103**: 4010–22.
2 Ren R. Mechanisms of BCR-ABL in the pathogenesis of chronic myelogenous leukaemia. *Nat Rev Cancer* 2005; **5**: 172–83.
3 Melo JV, Barnes DJ. Chronic myeloid leukaemia as a model of disease evolution in human cancer. *Nat Rev Cancer* 2007; **7**: 441–53.
4 Honda H, Oda H, Suzuki T *et al.* Development of acute lymphoblastic leukemia and myeloproliferative disorder in transgenic mice expressing p210bcr/abl: a novel transgenic model for human Ph1-positive leukemias. *Blood* 1998; **91**: 2067–75.
5 Honda H, Ushijima T, Wakazono K *et al.* Acquired loss of p53 induces blastic transformation in p210bcr/abl-expressing hematopoietic cells: a transgenic study for blast crisis of human CML. *Blood* 2000; **95**: 1144–50.
6 Niki M, Cristofano DA, Zhao M *et al.* Role of Dok-1 and Dok-2 in leukemia suppression. *J Exp Med* 2004; **200**: 1689–95.
7 Mizuno T, Yamasaki N, Miyazaki K *et al.* Overexpression/enhanced kinase activity of BCR/ABL and altered expression of Notch1 induced acute leukemia in p210BCR/ABL transgenic mice. *Oncogene* 2008; **29**: 3465–74.
8 Wakabayashi Y, Watanabe H, Inoue J *et al.* Bcl11b is required for differentiation and survival of αβ T lymphocytes. *Nat Immunol* 2003; **4**: 533–9.
9 Bonner WM, Redon CE, Dickey JS *et al.* γH2AX and cancer. *Nat Rev Cancer* 2008; **8**: 957–67.
10 Bassing CH, Chua KF, Sekiguchi J *et al.* Increased ionizing radiation sensitivity and genomic instability in the absence of histone H2AX. *Proc Natl Acad Sci USA* 2002; **99**: 8173–8.
11 Miyazaki K, Kawamoto T, Tanimoto K, Nishiyama M, Honda H, Kato Y. Identification of functional hypoxia response elements in the promoter region of the DEC1 and DEC2 genes. *J Biol Chem* 2002; **277**: 47 014–21.
12 Honda H, Ohno S, Takahashi T, Takatoku M, Yazaki Y, Hirai H. Establishment, characterization, and chromosomal analysis of new leukemic cell lines derived from MT/p210bcr/abl transgenic mice. *Exp Hematol* 1998; **26**: 188–97.
13 Harada H, Harada Y, Tanaka H, Kimura A, Inaba T. Implications of somatic mutations in the AML1 gene in radiation-associated and therapy-related myelodysplastic syndrome/acute myeloid leukemia. *Blood* 2003; **101**: 673–80.
14 Bassing CH, Suh H, Ferguson DO *et al.* Histone H2AX: a dosage-dependent suppressor of oncogenic translocations and tumors. *Cell* 2003; **114**: 359–70.
15 Celeste A, Difilippantonio S, Difilippantonio MJ *et al.* H2AX haploinsufficiency modifies genomic stability and tumor susceptibility. *Cell* 2003; **114**: 371–83.
16 Satterwhite E, Sonoki T, Willis TG *et al.* The BCL11 gene family: involvement of BCL11A in lymphoid malignancies. *Blood* 2001; **98**: 3413–20.
17 Wakabayashi Y, Inoue J, Takahashi Y *et al.* Homozygous deletions and point mutations of the Rit1/Bcl11b gene in gamma-ray induced mouse thymic lymphomas. *Biochem Biophys Res Commun* 2003; **301**: 598–603.
18 Albu DI, Feng D, Bhattacharya D *et al.* BCL11B is required for positive selection and survival of double-positive thymocytes. *J Exp Med* 2008; **204**: 3003–15.
19 Przybylski GK, Dik WA, Wanzeck J *et al.* Disruption of the BCL11B gene through inv (14) (q11.2q32.31) results in the expression of BCL11B-TRDC fusion transcripts and is associated with the absence of wild-type BCL11B transcripts in T-ALL. *Leukemia* 2005; **19**: 201–8.
20 Riches LC, Lynch AM, Gooderham NJ. Early events in the mammalian response to DNA double-strand breaks. *Mutagenesis* 2008; **23**: 331–9.
21 Kinner A, Wu W, Staudt C, Iliakis G. c-H2AX in recognition and signaling of DNA double-strand breaks in the context of chromatin. *Nucl Acids Res* 2008; **36**: 5678–94.
22 Novik KL, Spinelli JJ, Macarthur AC *et al.* Genetic variation in H2AFX contributes to risk of non-Hodgkin lymphoma. *Cancer Epidemiol Biomarkers Prev* 2007; **16**: 1098–106.
23 Kamimura K, Ohi H, Kubota T *et al.* Haploinsufficiency of Bcl11b for suppression of lymphomagenesis and thymocyte development. *Biochem Biophys Res Commun* 2007; **355**: 538–42.
24 Gishizky ML, Johnson-White J, Witte ON. Efficient transplantation of BCR-ABL-induced chronic myelogenous leukemia-like syndrome in mice. *Proc Natl Acad Sci USA* 1993; **90**: 3755–9.

© 2009 Japanese Cancer Association

Supporting information

Additional Supporting Information may be found in the online version of this article:

Fig. S1. Expression of *Bcl11b* and *H2AX* in chronic myelogenous leukemia (CML) chronic phase (CP), CML blast crisis (BC), and normal bone marrow (BM). RNA extracted from one CML CP sample, four CML BC samples (two myeloid and two B-lymphoid), and one normal BM sample were subjected to RT-PCR for the expression of *Bcl11b* and *H2AX*. *β-Actin* RT-PCR was carried out as an internal control.

Please note: Wiley-Blackwell are not responsible for the content or functionality of any supporting materials supplied by the authors. Any queries (other than missing material) should be directed to the corresponding author for the article.

doi: 10.1111/j.1349-7006.2009.01172.x
© 2009 Japanese Cancer Association

THE JOURNAL OF BIOLOGICAL CHEMISTRY VOL. 285, NO. 3, pp. 1850–1860, January 15, 2010
© 2010 by The American Society for Biochemistry and Molecular Biology, Inc. Printed in the U.S.A.

Up-regulation of Survivin by the E2A-HLF Chimera Is Indispensable for the Survival of t(17;19)-positive Leukemia Cells*

Received for publication, June 10, 2009, and in revised form, October 29, 2009 Published, JBC Papers in Press, November 2, 2009, DOI 10.1074/jbc.M109.023762

Mayuko Okuya[‡], Hidemitsu Kurosawa[‡1], Jiro Kikuchi[§], Yusuke Furukawa[§], Hirotaka Matsui[¶], Daisuke Aki[¶], Takayuki Matsunaga[‡], Takeshi Inukai[‖], Hiroaki Goto[**], Rachel A. Altura[‡‡], Kenich Sugita[‡], Osamu Arisaka[‡], A. Thomas Look[§§], and Toshiya Inaba[¶]

From the [‡]Department of Pediatrics, Dokkyo Medical University School of Medicine, Tochigi 321-0293, Japan, the [§]Division of Stem Cell Regulation Center for Molecular Medicine, Jichi Medical School, Tochigi 329-0498, Japan, the [¶]Department of Molecular Oncology, Research Institute for Radiation Biology and Medicine, Hiroshima University, Hiroshima 734-8553, Japan, the [‖]Department of Pediatrics, University of Yamanashi School of Medicine, Yamanashi 409-3898, Japan, the [**]Department of Pediatrics, Yokohama City University School of Medicine, Kanagawa 236-0004, Japan, the [‡‡]Department of Pediatrics, The Warren Alpert Medical School of Brown University, Providence, Rhode Island 02903, and the [§§]Pediatric Oncology Department, Dana-Farber Cancer Institute, Boston, Massachusetts 02115

The E2A-HLF fusion transcription factor generated by t(17;19)(q22;p13) translocation is found in a small subset of pro-B cell acute lymphoblastic leukemias (ALLs) and promotes leukemogenesis by substituting for the antiapoptotic function of cytokines. Here we show that t(17;19)$^+$ ALL cells express Survivin at high levels and that a dominant negative mutant of E2A-HLF suppresses Survivin expression. Forced expression of E2A-HLF in t(17;19)$^-$ leukemia cells up-regulated Survivin expression, suggesting that Survivin is a downstream target of E2A-HLF. Analysis using a counterflow centrifugal elutriator revealed that t(17;19)$^+$ ALL cells express Survivin throughout the cell cycle. Reporter assays revealed that E2A-HLF induces *survivin* expression at the transcriptional level likely through indirect down-regulation of a cell cycle-dependent *cis* element in the promoter region. Down-regulation of Survivin function by a dominant negative mutant of Survivin or reduction of Survivin expression induced massive apoptosis throughout the cell cycle in t(17;19)$^+$ cells mainly through caspase-independent pathways involving translocation of apoptosis-inducing factor (AIF) from mitochondria to the nucleus. AIF knockdown conferred resistance to apoptosis caused by down-regulation of Survivin function. These data indicated that reversal of AIF translocation by Survivin, which is induced by E2A-HLF throughout the cell cycle, is one of the key mechanisms in the protection of t(17;19)$^+$ leukemia cells from apoptosis.

The E2A-HLF fusion transcription factor, which is generated by the t(17;19)(q22;p13) translocation, is found in a small subset of pro-B cell acute lymphoblastic leukemias (ALLs)[2] that occurs in older children and adolescents (1, 2). In this chimeric molecule, the *trans*-activation domain of E2A is fused to the basic region and leucine zipper domain of HLF, which mediates DNA binding and dimerization. Patients with this chimera share distinct clinical features such as hypercalcemia and coagulopathy and very poor prognosis because of resistance to intensive chemotherapy, including aggressive conditioning for bone marrow transplantation (3–5), all of which are unusual for pro-B cell ALLs. Thus, these features may be a direct consequence of aberrant gene expression induced by E2A-HLF fusion transcription factor, rather than a consequence of the nature of B cell progenitors.

We previously demonstrated that inhibition of the *trans*-activation potential of the E2A-HLF chimera by a dominant negative mutant results in apoptosis in t(17;19)$^+$ ALL cells but does not affect the cell cycle (6). Moreover, E2A-HLF blocks apoptosis normally induced by cytokine deprivation in murine interleukin (IL)-3-dependent B precursor lines such as Baf-3 or FL5.12 cells, suggesting that this fusion protein contributes to leukemogenesis through modification of apoptosis regulatory pathways normally controlled by cytokines (6, 7). We speculated that the target genes of E2A-HLF involved in the inhibition of apoptosis are those regulated via Ras pathways in IL-3-dependent cells, because activation of Ras pathways is indispensable for long term survival of Baf-3 cells in cytokine-free medium (8, 9). Moreover, we previously identified E4BP4/NFIL3, a related basic region and leucine zipper factor with antiapoptotic function, as a possible physiological counterpart of E2A-HLF (10), and we found that E4BP4 expression is induced by IL-3 through Ras-phosphatidylinositol 3-kinase and Ras-Raf-MAPK pathways in IL-3-dependent cells (9).

The *survivin* gene may be a good candidate for a target gene of E2A-HLF involved in the inhibition of apoptosis in t(17;19)$^+$

* This work was supported by Grant-in-aid for Scientific Research (C) 18591201 from the Japan Society for Promotion of Science (to H. K.) and a young investigator award from Dokkyo Medical University (to M. O.).

[1] To whom correspondence should be addressed: Dept. of Pediatrics, Dokkyo Medical University, Mibu, Tochigi 321-0293, Japan. Tel.: 81-282-86-1111; Fax: 81-282-86-2947; E-mail: hidekuro@dokkyomed.ac.jp.

[2] The abbreviations used are: ALL, acute lymphoblastic leukemia; AIF, apoptosis-inducing factor; IL, interleukin; MAPK, mitogen-activated protein kinase; CHR, cell cycle homology region; PBS, phosphate-buffered saline; FITC, fluorescein isothiocyanate; shRNA, short hairpin RNA; siRNA, short interfering RNA; GFP, green fluorescent protein; EMSA, electrophoretic mobility shift assay; BrdUrd, bromodeoxyuridine; TdT, terminal deoxynucleotidyltransferase; PARP, poly(ADP-ribose) polymerase; TUNEL, terminal deoxynucleotidyltransferase-mediated dUTP nick-end-labeling; PI, propidium iodide; dn, dominant negative; nt, nucleotide; 7-AAD, 7-amino-actinomycin D; PLL, plenti-Lox3.7.

Downloaded from www.jbc.org at HIROSHIMA UNIVERSITY, on May 10, 2010

ALL cells. Survivin, at 142 amino acids, is the smallest member of the inhibitor of apoptosis protein family and significantly prolongs the viability of cytokine-deprived IL-3-dependent cells (11). The expression of Survivin is controlled by oncogenic c-H-ras, and up-regulation of Survivin depends on functional Ras/phosphatidylinositol 3-kinase and Ras-Raf-MAPK signaling pathways (12). Overexpression of Survivin can protect cells from both extrinsically and intrinsically induced apoptosis (13, 14), whereas inhibition of Survivin expression by antisense ribozyme or RNA interference leads to increased spontaneous apoptosis (15, 16).

A unique feature of Survivin as an apoptosis regulator is its involvement in cell cycle progression (17). *survivin* expression is transcriptionally induced in the G_2/M phase through cell cycle-dependent *cis* elements located near the transcription initiation site (16). These elements, including the cell cycle-dependent element (GGCGG) and the cell cycle homology region (CHR; ATTTGAA), are implicated in G_1 transcriptional repression in S/G_2-regulated genes, such as cyclin A, cdc25C, and cdc2 (18). In addition, Survivin is activated through phosphorylation of Thr-34 by mitotic kinase CDC2-cyclin-B1 (14). Enforced expression of a phosphorylation-defective Survivin T34A mutant (Survivin-T34A) initiates mitochondrial dependent apoptosis in a variety of tumor cell lines (14, 16).

Here, we show that Survivin expression is induced by the E2A-HLF chimera, and down-regulation of Survivin induces caspase-independent massive apoptosis in t(17;19)$^+$ ALL cell lines. These findings indicate that Survivin contributes to leukemogenesis by subverting genetic pathways responsible for the apoptosis of B cell progenitors.

EXPERIMENTAL PROCEDURES

Cell Lines and Cell Culture—Human ALL cell lines that express E2A-HLF (UOC-B1, HAL-O1, YCUB-2, and Endo-kun) and other leukemia cell lines (Nalm-6, RS4;11, REH, 697, 920, HL-60, NB-4, and Jurkat) were cultured in RPMI 1640 medium containing 10% fetal bovine serum. Establishment of Nalm-6 human pro-B cell leukemia cells that express zinc-inducible E2A-HLF (Nalm-6/E2A-HLF) using the pMT-CB6$^+$ eukaryotic expression vector (a gift from Dr. F. Rauscher III, Wistar Institute, Philadelphia) has been described previously (19). UOC-B1/E2A-HLF(dn) cells transfected with a dominant negative mutant of E2A-HLF, which lacks the AD1 transactivation domain of E2A and contains a mutated HLF DNA-binding domain with an intact leucine-zipper domain, were prepared as described previously (6). UOC-B1, Endo-kun, REH, and Jurkat cells that were transfected with either the pMT/Survivin-T34A vector or the empty pMT-CB6$^+$ vector were designated as UOC-B1/Survivin(dn), UOC-B1/pMT, Endo-kun/Survivin(dn), Endo-kun/pMT, REH/Survivin(dn), REH/pMT, Jurkat/Survivin(dn), and Jurkat/pMT, respectively.

Counterflow Centrifugal Elutriations—Counterflow centrifugal elutriations were performed using the SRR6Y elutriation system and rotor equipped with a 4.5-ml chamber (Hitachi Koki Co., Ltd., Tokyo, Japan) (20). Target cells were resuspended at 1–2 × 10^8 cells in 50 ml of PBS containing 1% fetal bovine serum and injected into the elutriation system at 4 °C using an initial flow rate of 16 ml/min and rotor speed of 2,000 rpm. The flow rate was incrementally increased, and cell fractions were collected serially as follows: fraction 1, 200 ml at 16 ml/min; fraction 2, 200 ml at 18 ml/min; fraction 3, 200 ml at 20 ml/min; fraction 4, 200 ml at 22 ml/min; fraction 5, 200 ml at 24 ml/min; fraction 6, 200 ml at 26 ml/min; and fraction 7, 200 ml at 28 ml/min. Cell cycle analysis was performed on each fraction by staining DNA with propidium iodide (PI) in preparation for flow cytometry with the FACScan/CellFIT system (BD Biosciences).

Gene Silencing by RNA Interference—Short hairpin/short interfering RNA (shRNA/siRNA) was introduced into UOC-B1 or UOC-B1/Survivin(dn) cells to down-regulate the expression of Survivin or apoptosis-inducing factor (AIF) by the shRNA lentivirus system (21, 22). Oligonucleotides were chemically synthesized, annealed, terminally phosphorylated, and inserted into the vector pLL3.7 (Addgene, Cambridge, MA). Oligonucleotides containing siRNA target for *survivin* sequences (23) were as follows: 5′-TGAAGCGTCTGGCAGATACTTTCAAGAGAAGTATCTGCCAGACGCTTCTTTTTTC-3′ (forward 1) and 5′-TCGAGAAAAAAGAAGCGTCTGGCAGATACTTCTCTTGAAAGTATCTGCCAGACGTTCA-3′ (reverse 1); 5′-TGTGGATGAGGAGACAGAATTTCAAGAGAATTCTGTCTCCTCATCCACTTTTTTC-3′ (forward 3) and 5′-TCGAGAAAAAAGTGGATGAGGAGACAGAATTCTCTTGAAATTCTGTCTCCTCATCCACA-3′ (reverse 3); 5′-TGGATACTTCACTTTAATAATTCAAGAGATTATTAAAGTGAAGTATCCTTTTTTC-3′ (forward 4) and 5′-TCGAGAAAAAAGGATACTTCACTTTAATAATCTCTTGAATTATTAAAGTGAAGTATCCA-3′ (reverse 4); 5′-TGCTTCCTCGACATCTGTTATTCAAGAGATAACAGATGTCGAGGAAGCTTTTTTC-3′ (forward 5) and 5′-TCGAGAAAAAAGCTTCCTCGACATCTGTTATCTCTTGAATAACAGATGTCGAGGAAGCA-3′ (reverse 5). Oligonucleotides containing siRNA target for *AIF* sequences were as follows: 5′-TGGAGGAGTCTGCGTAATGTTTCAAGAGAACATTACGCAGACTCCTCCTTTTTTC-3′ (forward 1) and 5′-TCGAGAAAAAAGGAGGAGTCTGCGTAATGTTCTCTTGAAACATTACGCAGACTCCTCCT-3′ (reverse 1); 5′-TGCAGGAAGGTAGAAACTGATTCAAGAGATCAGTTTCTACCTTCCTGCTTTTTTC-3′ (forward 2) and 5′-TCGAGAAAAAAGCAGGAAGGTAGAAACTGATCTCTTGAATCAGTTTCTACCTTCCTGCT-3′ (reverse 2); 5′-TGCATGCTTCTACGATATAATTCAAGAGATTATATCGTAGAAGCATGCTTTTTTC-3′ (forward 3) and 5′-TCGAGAAAAAAGCATGCTTCTACGATATAATCTCTTGAATTATATCGTAGAAGCATGCT-3′ (reverse 3); the nucleotide sequences corresponding to the siRNA are underlined. The resulting plasmids or the parental pLL3.7, along with lentiviral packaging mix (ViraPower, Invitrogen), was transfected into 293FT cells (Invitrogen) to produce recombinant lentivirus, and the UOC-B1 or UOC-B1/Survivin(dn) cells were infected with the virus. Enhanced green fluorescent protein (GFP)-positive cells were purified by FACSAria (BD Biosciences) as shRNA-transfected cell populations.

Reporter Assay—Fragments of the 5′-flanking region of the human *survivin* gene spanning 147, 213, 288, 503, or 698 bp were generated by PCR using *Pfu* polymerase from genomic DNA of human placenta. The positions of the forward (5′)

Downloaded from www.jbc.org at HIROSHIMA UNIVERSITY, on May 10, 2010

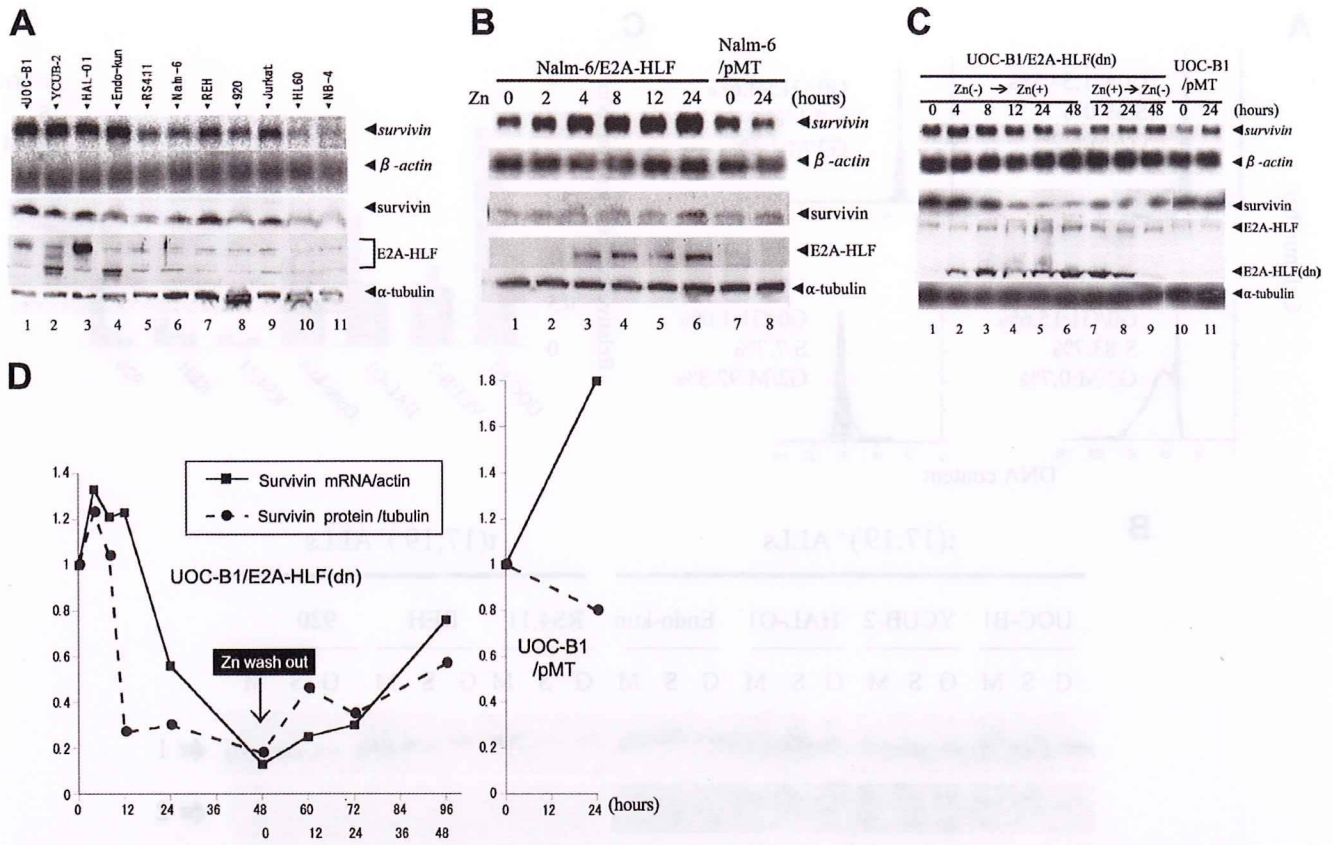

FIGURE 1. **Expression of Survivin in human leukemia cell lines and induction of Survivin by E2A-HLF in human ALL cells.** *A, top 2 panels,* Northern blot analysis of poly(A)$^+$ RNA isolated from human leukemia cell lines. The blot was hybridized with a *survivin* cDNA probe and then rehybridized with a β-actin probe. *Lower three panels,* immunoblot analysis using whole-cell lysates. Survivin, E2A-HLF, and α-tubulin proteins were detected with specific antibodies. *Lanes 1–4,* the UOC-B1, YCUB-2, HAL-O1, and Endo-kun t(17;19)-positive pro-B ALL cell lines; *lanes 5–8,* the RS4;11, Nalm-6, REH, and 920 pro-B ALL cell lines without t(17;19); *lane 9,* the Jurkat T-ALL cell line; *lane 10,* the HL-60 AML cell line; and *lane 11,* the NB-4 APL cell line. *B,* Nalm-6 cells with zinc-inducible expression of E2A-HLF (Nalm-6/E2A-HLF) and control Nalm-6/pMT cells were cultured in medium containing 100 μM zinc for the indicated length of time. *C* and *D,* UOC-B1 cells with zinc-inducible expression of E2A-HLF(dn) (UOC-B1/E2A-HLF(dn)) and control UOC-B1/pMT cells were cultured in medium containing 100 μM zinc for the indicated length of time (*Zn*(−) → *Zn*(+)) and removal of zinc from the growth medium (*Zn*(+) → *Zn*(−)). *C, upper two panels,* Northern blot analysis of poly(A)$^+$ RNA. The blot was hybridized with a *survivin* cDNA probe and then rehybridized with a β-actin probe. *Lower three panels,* immunoblot analysis for Survivin, E2A-HLF, or α-tubulin proteins. *D,* quantification of intensity of each band.

primers with respect to the translational initiation codon (according to NCBI GenBank™ sequence U75285) are −124 (−124 forward primer, 5′-ACTCCCAGAAGGCCGCGGGG-GGTG-3′), −190 (5′-ACCACGGGCAGAGCCACGCGGC-GGG-3′), −265 (5′-GTTCTTTGAAAGCAGTCGAGGGGGC-3′), −480 (5′-CGGGTTGAAGCGATTCTCCTGCCT-3′), and −675 (5′-CGATGTCTGCACTCCATCCCTC-3′). The reverse (3′) primer used for these amplifications was at position 23 (+23-reverse primer, 5′-GGGGGCAACGTCGGGGCAag-CtTGC-3′) and was constructed based on the genomic sequence with a modification (lowercase) to create a HindIII site. The PCR products were cloned into a pGL3-basic vector (Promega, Madison, WI). The resulting reporter plasmids were designated as pGL3-124, pGL3-190, pGL3-265, pGL3-480, and pGL3-675, respectively. The pGL3-124mut1 vector containing two mutated cell cycle-dependent elements (−6 and −12) was generated by PCR using the −124 forward primer and a reverse primer (5′-GCAAGCTTGtcactGtcactACCTCTG-3′); pGL3-124mut2 vector containing mutated CHR (−42) in addition to two mutated cell cycle-dependent elements (−6 and −12) was generated by the −124 forward primer and a reverse primer (5′-GCAAGCTTGtcactGtcactACCTCTGCCAACGGGTCC-CGCGATTCgggTCTGG-3′); and pGL3-124mut3 vector containing a mutated CHR (−42) was generated by the −124 forward primer and a reverse primer (5′-GCAAGCTTGCCGCC-GCCGCCACCTCTGCCAACGGGTCCCGCGATTCgggTC-TGG-3′) (lowercase indicates mutations).

For transfection with a pMT-CB6$^+$/E2A-HLF construct, Nalm-6 cells (6×10^4) were seeded into 24-well plates, cotransfected with pGL3-*survivin* promoter construct plus pRL-TK vector, which contains the *Renilla* luciferase gene, by Lipofectamine 2000 (Invitrogen), and harvested 24 h later. E2A-HLF expression was induced in Nalm-6 cells by the addition of 100 μM $ZnCl_2$ 24 h after transfection. Firefly luciferase and *Renilla* luciferase as a transfection efficiency control were detected with Dual-Luciferase Reporter Assay System (Promega) according to the manufacturer's instructions and measured in a Veritas Microplate Luminometer (Promega).

Electrophoretic Mobility Shift Assays (EMSA)—EMSA were performed by incubating 12 μg of nuclear protein lysate at 30 °C for 15 min with a ^{32}P-end-labeled DNA oligonucleotide probe (2×10^4 cpm) containing the CHR-binding site sequence

Downloaded from www.jbc.org at HIROSHIMA UNIVERSITY, on May 10, 2010

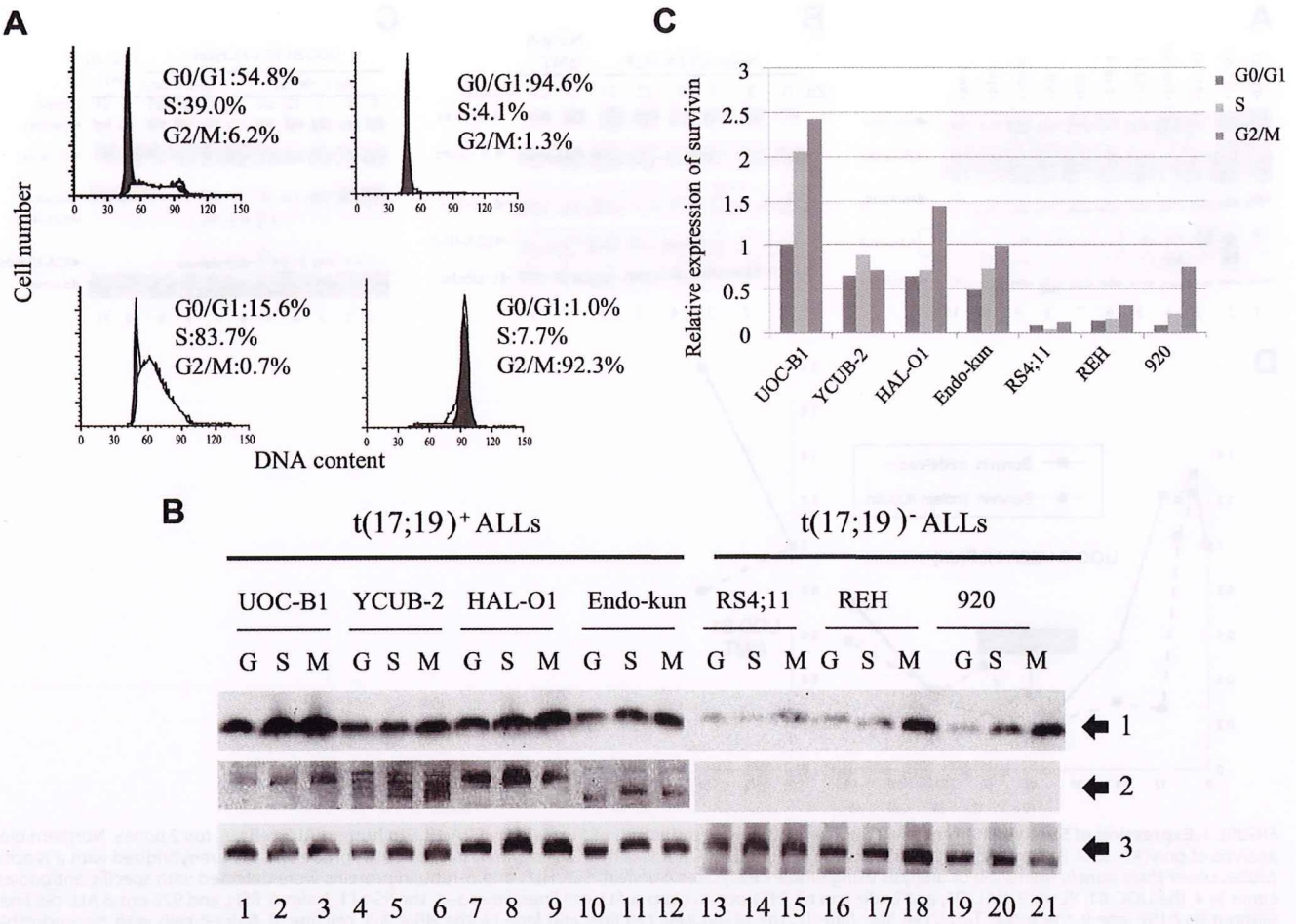

FIGURE 2. **Cell cycle-dependent and -independent expression of Survivin in human leukemia cells.** Fractions enriched with cells at each phase of the cell cycle were separated by counterflow centrifugal elutriation. *A*, representative DNA histogram of each fraction subjected to flow cytometry after staining DNA with PI. *Upper left*, no fractionation; *upper right*, G_0/G_1 phase-enriched fraction; *lower left*, S-phase-enriched fraction; *lower right*, G_2/M-phase-enriched fraction. *B*, immunoblot analysis of fractions of t(17;19)$^+$ ALL cells or t(17;19)$^-$ ALL cells enriched with cells in the G_0/G_1- (*G*), S- (*S*), or G_2/M (*M*)-phase. Survivin (*arrow 1*), E2A-HLF (*arrow 2*), and α-tubulin (*arrow 3*) proteins were detected with specific antibodies. *C*, levels of Survivin and α-tubulin proteins were determined by the band intensity on autoradiograms from *B*. Levels of Survivin were normalized to levels of α-tubulin, and amounts shown are relative to amounts in UOC-B1 cells in the G_0/G_1-phase.

in the *survivin* promoter (5′-CATTAACCGCCAGATTTGAATCGCGG-3′) in a solution of 12% glycerol, 12 mM HEPES (pH 7.9), 4 mM Tris (pH 7.9), 133 mM KCl, 1.5 μg of sheared calf thymus DNA, and 300 μg of bovine serum albumin per ml as described previously (24). In the competitive inhibition experiments, excess of the unlabeled CHR-consensus sequence probe, *i.e.* oligonucleotide containing the candidate-binding sites of CHR in the *survivin* gene promoter or its 3-bp mismatched oligonucleotide (5′-CATTAACCGCCAGAcccGAATCGCGG-3′) was added to the reaction mixture. The entire mixture was incubated at 30 °C for 15 min. Nondenaturing polyacrylamide gels containing 4% acrylamide and 2.5% glycerol were prerun at 4 °C in a high ionic strength Tris-glycine buffer for 30 min and run at 50 mA for ~45 min. The gel was then dried under vacuum and analyzed by autoradiography.

Other Experimental Procedures—For visualization of intracellular AIF, cytospinned cells were fixed with 1% paraformaldehyde in PBS for 10 min, and permeabilized with 0.5% Triton X-100 in PBS for 5 min. Cells were rinsed twice with PBS (5 min for each rinse), blocked with 5% goat serum in PBS for 30 min, and incubated with anti-AIF antibody (1:100; Santa Cruz Biotechnology, Santa Cruz, CA) overnight at 4 °C in a humidified chamber. Cells were incubated with a secondary antibody, fluorescein isothiocyanate (FITC)-labeled anti-goat IgG (1:500; Santa Cruz Biotechnology), at 37 °C for 30 min.

For Northern blot analysis, 1 μg of poly(A)-selected RNA was separated by electrophoresis in 1% agarose gels containing 2.2 M formaldehyde, transferred to nylon membranes, and hybridized with the appropriate probe according to standard procedures as described previously (5). For immunoblot analysis, the primary antibodies used were anti-Survivin polyclonal (R & D Systems, Minneapolis, MN), anti-α-tubulin monoclonal (Sigma), anti-caspase 3 polyclonal (Cell Signaling Technology, Beverly, MA), anti-caspase 9 polyclonal (BD Biosciences), anti-PARP monoclonal (BD Biosciences), and anti-AIF polyclonal antibodies (Santa Cruz Biotechnology). Anti-HLF(C) antibody for detection of the E2A-HLF chimeric protein was described previously (24).

Cell viability was determined by trypan blue dye exclusion. Early apoptotic events were detected by flow cytometric mea-

Downloaded from www.jbc.org at HIROSHIMA UNIVERSITY, on May 10, 2010

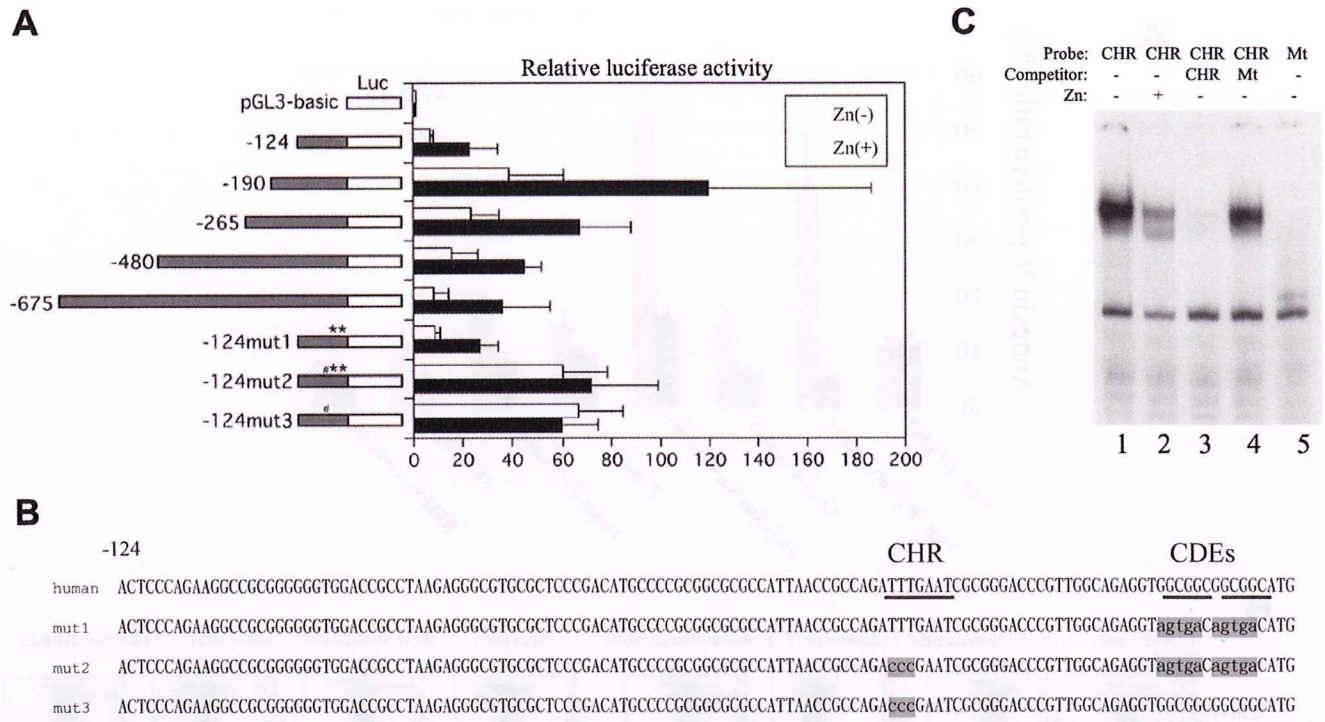

FIGURE 3. **Effect of E2A-HLF on *survivin* promoter activity in transiently transfected t(17;19)$^-$ ALL cells.** *A*, Nalm-6/E2A-HLF cells cotransfected with pRL-TK vector and the pGL3-*survivin* promoter constructs indicated at the *left* were cultured in the absence (*open bars*) or presence (*black bars*) of zinc for 24 h. Firefly luciferase (*Luc*) activity was normalized to *Renilla* luciferase as a transfection efficiency control. The level of activity of the promoterless *Renilla* plasmid luciferase was defined as 1. The results depicted are the averages of three independent experiments; *error bars* indicate S.D. # indicates mutation of CHR, and ** indicates mutation of CDE. *B*, nucleotide sequences of the human *survivin* promoter and three mutants. *Underlines* indicate CHR or CDE region. *Shaded characters* indicate mutation (*mut*). *C*, EMSA. Nuclear lysates extracted from Nalm-6/E2A-HLF cells cultured without (*lanes 1* and *3–5*) or with zinc (*lane 2*) were incubated with a ^{32}P-end-labeled oligonucleotide probe containing the CHR sequence (*lanes 1–4*) or mutated CHR sequence (*lane 5*). An excess of unlabeled CHR sequence competitor (*lane 3*) or mutant competitor (*lane 4*) was added to the reaction mixture. *Mt*, mutant.

surement of externalized phosphatidylserine with the annexin-V-FITC apoptosis detection kit I (BD Biosciences) in preparation for flow cytometry with the FACScan/CellFIT system (BD Biosciences). For caspase inhibition, 20 μM benzyloxycarbonyl-VAD-fluoromethyl ketone (BD Biosciences) was added to the cells 1 h before the addition of zinc. Terminal deoxynucleotidyltransferase-mediated dUTP nick-end-labeling (TUNEL) was performed using the apo-BrdUrd TUNEL assay kit (Molecular Probes, Eugene, OR). Briefly, cells fixed with paraformaldehyde and ethanol were incubated with BrdUrd and TdT for 1 h at 37 °C. BrdUrd uptakes were detected by Alexa dye-leveled anti-BrdUrd antibodies. Cells were stained by PI just before analysis using FACScan/CellFIT system.

RESULTS

E2A-HLF Regulates Survivin Expression—Cell lines were used in this study instead of primary patient samples, because t(17;19)$^+$ ALLs constitute only ~1% of childhood B-precursor ALLs (1–3). Four t(17;19)$^+$ ALL cell lines (UOC-B1, YCUB-2, HAL-O1, and Endo-kun) expressed the E2A-HLF chimeric protein on immunoblot analysis (Fig. 1*A*, *4th panel, lanes 1–4*) either as a slower (*lanes 1* and *3*) or a faster migration band (*lanes 2* and *4*) corresponding to difference in the fusion junction, as described previously (3). Of the seven t(17;19)$^-$ leukemia cell lines tested (RS4;11, Nalm-6, REH, 920, Jurkat, HL-60 and NB-4), none expressed the E2A-HLF chimera (Fig. 1*A*, *lanes 5–11*). We performed Northern blot and immunoblot analyses to test human leukemia cell lines for the expression of *survivin*. Survivin mRNA and protein were expressed at uniformly high levels in the four t(17;19)$^+$ ALL cell lines (Fig. 1*A*, *top* and *3rd panels*). By contrast, *survivin* mRNA levels varied among the t(17;19)$^-$ leukemia cell lines and appeared to determine Survivin protein expression levels in each line (Fig. 1*A*, *lanes 5–11*).

Next, we tested whether E2A-HLF induces the expression of Survivin. For these experiments, Nalm-6 cells were transfected with a pMT-CB6+/E2A-HLF construct to generate clones (Nalm-6/E2A-HLF) with zinc-inducible expression of E2A-HLF (Fig. 1*B*, *4th panel*). Ectopic expression of E2A-HLF in Nalm-6 cells induced *survivin* mRNA by 5-fold within 24 h after the addition of zinc (Fig. 1*B*, *top panel*). Accordingly, Survivin protein expression increased within 24 h after induction of E2A-HLF (Fig. 1*B*, *3rd panel*). In control Nalm-6/pMT cells, which contained the empty vector, Survivin expression was unaffected by zinc (Fig. 1*B*, *lanes 7* and *8*), confirming that the observed changes in Survivin expression were induced by E2A-HLF and not by zinc.

Induction of Survivin by E2A-HLF was further confirmed using UOC-B1/E2A-HLF(dn) cells, which express zinc-inducible E2A-HLF(dn), a dominant negative mutant of E2A-HLF (see under "Experimental Procedures") (6, 19). Survivin mRNA and protein expression in UOC-B1/E2A-HLF(dn) cells were high in the absence of zinc (Fig. 1*C*, *top* and *3rd panels, lane 1*; see also Fig. 1*D*) but decreased within 24 h after the addition of

Downloaded from www.jbc.org at HIROSHIMA UNIVERSITY, on May 10, 2010

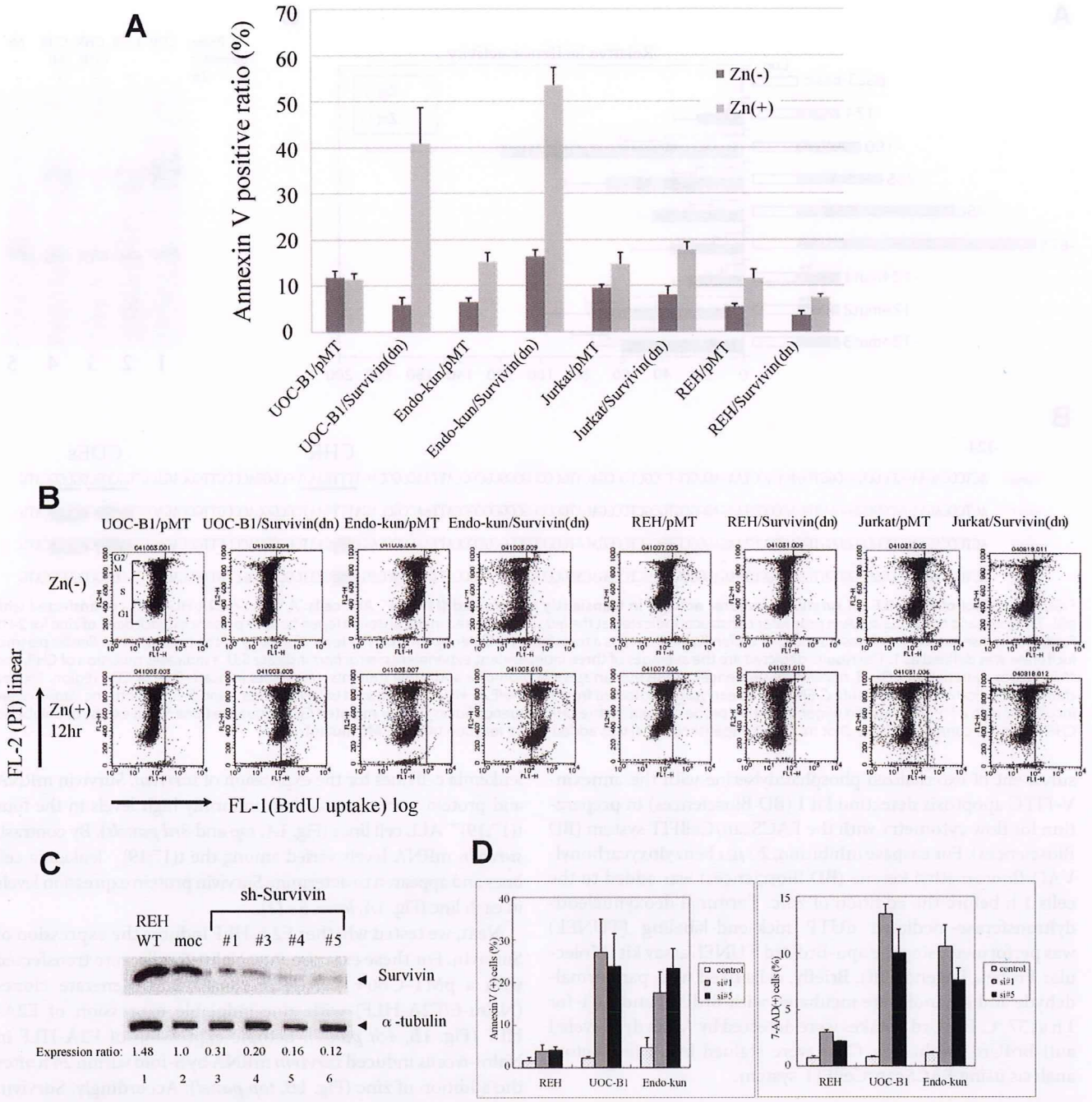

FIGURE 4. **Effect of enforced overexpression of Survivin-T34A and introduction of Survivin-shRNA in ALL cells.** UOC-B1, Endo-kun, Jurkat, and REH cells inducibly expressing Survivin-T34A (UOC-B1/Survivin(dn), Endo-kun/Survivin(dn), Jurkat/Survivin(dn) and REH/Survivin(dn) cells, respectively) were compared with control UOC-B1/pMT, Endo-kun/pMT, Jurkat/pMT, and REH/pMT cells, respectively. *A*, externalization of phosphatidylserine as determined by annexin-V binding. Cells cultured in medium with or without 100 μM zinc for 24 h were simultaneously stained with FITC-annexin-V and PI. The FITC-annexin-V-positive ratios were determined by representative flow cytometric plots. *B*, cells cultured in medium with or without 100 μM zinc for 12 h were simultaneously stained with PI and BrdUTP in a TdT-catalyzed reaction and then subjected to flow cytometric analysis. DNA ends labeled with BrdUTP (*abscissa*) are shown as a function of cellular DNA content of PI-stained nuclei (*ordinate*). Cells to the *right* of the *vertical line* had free DNA ends labeled with TdT, indicating apoptosis. Range of each cell cycle was shown in the panel of UOC-B1/pMT, *Zn*(−). *C*, immunoblot analyses using Survivin (*upper panel*) and α-tubulin (*lower panel*) antibodies. REH cells without treatment (*lane 1*) or infected with lentivirus (*lanes 2–6*) were sorted by GFP expression. *moc* indicates control sh-RNA. Ratios of intensity are shown *below*. *WT*, wild type. *D*, ratios of annexin-V-phycoerythrin (*PE*) (*left*) or 7-AAD (*right*)-positive cells in the GFP-positive fraction of REH, UOC-B1, or Endo-kun cells infected with lentivirus expressing GFP alone (control) or GFP and Survivin shRNA1 or -5 (*si#1* or *si#5*, respectively). Mean values from three independent experiments are shown with standard error.

zinc (Fig. 1*C*, *lane 5*), coincident with expression of E2A-HLF(dn) protein (*4th panel*). Removal of zinc from the growth medium restored Survivin expression within 48 h, again coincident with a decline in the E2A-HLF(dn) protein level (Fig. 1*C*, *lane 9*). These data suggested that E2A-HLF induces Survivin mRNA expression. Down-regulation of Survivin protein pre-

Downloaded from www.jbc.org at HIROSHIMA UNIVERSITY, on May 10, 2010

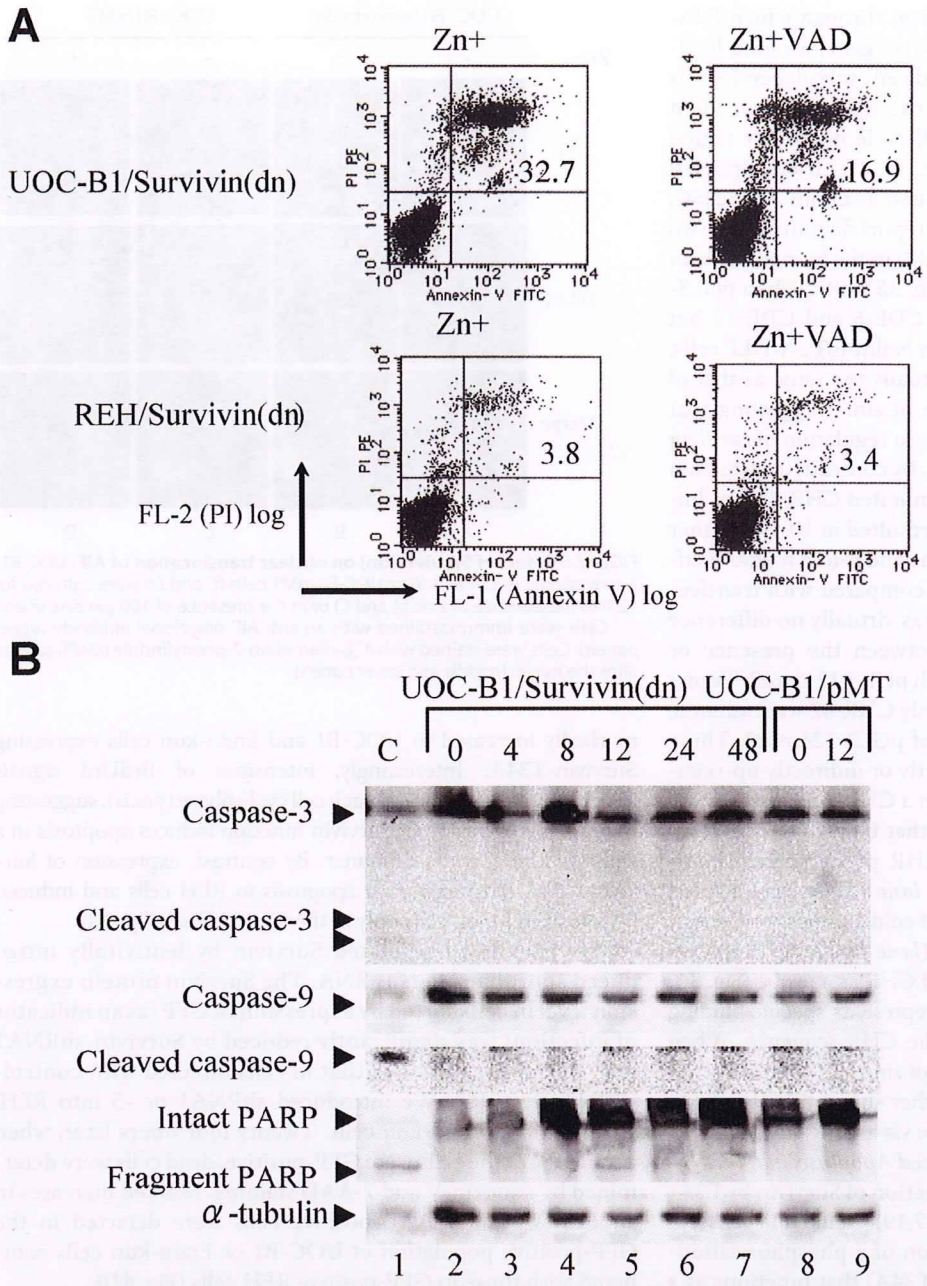

FIGURE 5. **PARP activation in Survivin(dn)-expressing cells and effect of caspase inhibitor.** *A*, flow cytometric analysis stained with annexin-V (*abscissa*) and PI (*ordinate*). UOC-B1/Survivin(dn) and REH/Survivin(dn) cells were cultured in medium containing 100 μM zinc 1 h after treatment with or without 20 μM benzyloxycarbonyl-VAD-fluoromethyl ketone (*VAD*), a pan-caspase inhibitor. *B*, UOC-B1/Survivin(dn) or UOC-B1/pMT cells were cultured in medium containing 100 μM zinc for the indicated times. Immunoblot analysis of UOC-B1/Survivin(dn) cells was performed to detect caspase-3, cleaved caspase-3, caspase-9, cleaved caspase-9, intact PARP, fragmented PARP, and α-tubulin proteins. As a positive control (*C*), Jurkat cells were treated with etoposide.

ceded the reduction of Survivin mRNA (Fig. 1*D*), suggesting the involvement of post-transcriptional mechanism(s).

Cell Cycle-independent Induction of Survivin by E2A-HLF—The Survivin mRNA and protein levels at the G_2/M phase of the cell cycle are more than 10-fold higher than those at the G_1 phase in NIH3T3 murine fibroblasts synchronized by serum starvation and in drug-synchronized HeLa cells (17, 25). Because it is difficult to synchronize leukemia cells by serum starvation or by reagents inhibiting cell cycle progression at a specific phase, we performed counterflow centrifugal elutriation to enrich cells at each phase of the cell cycle. The purity of the preparations was typically more than 90% for G_0/G_1-phase cells, more than 80% for S-phase cells, and ~90% for G_2/M-phase cells (Fig. 2*A*). We performed immunoblot analysis to measure Survivin expression in the enriched fractions. In t(17;19)$^-$ ALL cell lines (RS4;11, REH, and 920), Survivin expression was most evident at the G_2/M-phase (Fig. 2, *B*, *lanes 13–21*, and *C*). In particular, 920 cells at the G_2/M phase showed ~11- and 4-fold higher expression than those at the G_1 and S phase, respectively. By contrast, the four cell lines harboring the E2A-HLF chimeric protein expressed Survivin at high levels throughout the cell cycle (Fig. 2, *B*, *lanes 1–12*, and *C*).

E2A-HLF Enhances the Promoter Activity of the Survivin Gene—To elucidate how E2A-HLF induces expression of the *survivin* gene, we analyzed the effects of E2A-HLF on the function of the *survivin* promoter. We initially generated reporter plasmid vectors (pGL3-124, -190, -265, -480, and -675), each of which contained a different length of human *survivin* promoter. These vectors were analyzed for luciferase activity in transiently transfected Nalm-6/E2A-HLF cells. When cells were cultured without zinc, luciferase activity was low in cells transfected with pGL3-124 (Fig. 3*A*). Transfection of pGL3-190 resulted in the highest luciferase activity; it was nearly 6-fold higher than that which resulted from transfection of pGL3-124. However, transfection of *survivin* constructs longer than pGL3-265 resulted in significantly less activity compared with that of pGL3-190, suggesting the presence of enhancer elements in the region from nt −124 to −190 and repressor elements in the region upstream of nt −190. When cells were cultured with zinc for 24 h, the luciferase activity of each reporter construct, including the shortest pGL3-124, increased by ~3-fold compared with the respective cells cultured without zinc, suggesting that E2A-HLF induces *survivin* transcription through *cis* elements in the region from nt 0 to −124.

Downloaded from www.jbc.org at HIROSHIMA UNIVERSITY, on May 10, 2010

To further investigate the mechanism through which E2A-HLF induces transcription of the *survivin* gene, we used luciferase reporter constructs with mutated cell cycle-dependent *cis* elements. These elements, including the cell cycle-dependent element (CDE; GGCGG) and the cell cycle homology region (CHR; ATTTGAA), are implicated in G_1 transcriptional repression in S/G_2-regulated genes, such as cyclin A, cdc25C, and cdc2 (18). A previously published report demonstrated two CDEs (−6 and −12) and one CHR (−42) in the human *survivin* promoter between nt 0 and −124 (Fig. 3*B*) (18). When pGL3-124mut1, which contained mutated CDE-6 and CDE-12 but had intact CHR-42, was transfected in Nalm-6/E2A-HLF cells, the level of luciferase activity was virtually the same as that of pGL3-124 regardless of the presence of zinc, suggesting that CDE-6 and CDE-12 do not contribute to regulation of *survivin* transcription in Nalm-6 cells (Fig. 3*A*). By contrast, transfection of pGL3-124mut2, which contained mutated CHR-42 in addition to mutated CDE-6 and CDE-12, resulted in 10-fold higher luciferase activity in the absence of zinc and 3-fold higher luciferase activity in the presence of zinc compared with transfection of pGL3-124. As a result, there was virtually no difference in the level of luciferase activity between the presence or absence of zinc in cells transfected with pGL3-124mut2. Transfection of pGL3-124mut3, in which only CHR-42 was mutated, show similar results as transfection of pGL3-124mut2. These results suggested that E2A-HLF directly or indirectly up-regulates transcription of *survivin* through a CHR-42 silencer.

To elucidate transcription factors that bind to CHR-42, we performed EMSA. Smear-looking CHR probe-protein complexes were readily detected (Fig. 3*C*, *lane 1*) and were ablated by the addition of an excess amount of cold competitor (*lane 3*) but not by mutated CHR competitor (*lane 4*). These complexes were not detected when using mutated CHR as a probe (Fig. 3*C*, *lane 5*), suggesting that this complex represents specific binding between transcription factor(s) and the CHR sequence. When E2A-HLF was induced by the addition of zinc, the intensity of the smear decreased (Fig. 3*C*, *lane 2*), further supporting that E2A-HLF up-regulates expression of *survivin* via a CHR-42 silencer.

Specific Inhibition of Survivin-induced Apoptosis in t(17;19)$^+$ ALL Cell Lines—To test whether induction of Survivin by E2A-HLF is essential for the survival of t(17;19)$^+$ leukemia cells, we initially used zinc-inducible expression of a phosphorylation-defective Survivin mutant (Survivin-T34A) that functions as a dominant negative inhibitor. An annexin-V binding assay was used to measure externalization of phosphatidylserine, an indicator of cell death. Ectopic expression of Survivin-T34A in two t(17;19)$^+$ ALL cell lines (UOC-B1 and Endo-kun) caused a rapid increase in the fraction of annexin-V-positive cells within 24 h after the addition of zinc (Fig. 4*A*). In control UOC-B1/pMT and Endo-kun/pMT cells, which contained the empty vector, less than 20% of cells were positive for annexin-V regardless of the presence of zinc. By contrast, Survivin-T34A did not induce massive cell death in two t(17;19)$^-$ leukemia cell lines (REH and Jurkat), which express relatively high levels of Survivin (Fig. 1*A*). The basis for the altered survival of UOC-B1 and Endo-kun cells expressing Survivin-T34A was investigated by TUNEL analysis using flow cytometry. BrdUrd uptake (Fig. 4*B*, *x* axis) by TdT that reflects a number of DNA ends in each cell was markedly increased in UOC-B1 and Endo-kun cells expressing Survivin-T34A. Interestingly, intensities of BrdUrd signals increased equally in cells at each cell cycle phase (*y* axis), suggesting that down-regulation of Survivin function induces apoptosis in a cell cycle-independent manner. By contrast, expression of Survivin-T34A did not induce apoptosis in REH cells and induced apoptosis in Jurkat cells only at the G_2/M phase (Fig. 4*B*).

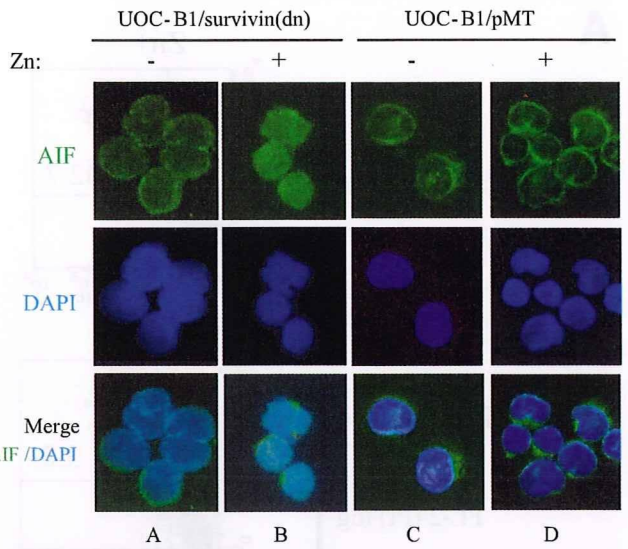

FIGURE 6. **Effect of Survivin(dn) on nuclear translocation of AIF.** UOC-B1/Survivin(dn) cells (*A* and *B*) or UOC-B1/pMT cells (*C* and *D*) were cultured for 12 h in the absence of zinc (*A* and *C*) or in the presence of 100 μM zinc (*B* and *D*). Cells were immunostained with an anti-AIF polyclonal antibody (*upper panels*). Cells were stained with 4′,6-diamidino-2-phenylindole (*DAPI*) to visualize the nuclei (*middle* and *lower panels*).

We next down-regulated Survivin by lentivirally introduced short hairpin (sh) RNA. The Survivin protein expression level in cells sorted by expression of GFP (as an indicator of infection) was significantly reduced by Survivin-shRNA1 and -3–5 compared with that in cells infected with control-shRNA (Fig. 4*C*). We introduced shRNA1 or -5 into REH, UOC-B1, and Endo-kun cells. Twenty four hours later, when about 10% of the cells were GFP-positive, dead cells were determined by annexin-V and 7-AAD staining. Marked increases in annexin-V- and 7-AAD-positive cells were detected in the GFP-positive population of UOC-B1 or Endo-kun cells compared with those in GFP-positive REH cells (Fig. 4*D*).

Caspase-dependent and -independent Cell Death Are Induced by Survivin-T34A in t(17;19)$^+$ Cells—To elucidate the molecular mechanisms through which Survivin protects t(17;19)$^+$ ALL cells from apoptosis, we initially examined caspase-dependent pathways. A pan-caspase inhibitor, benzyloxycarbonyl-VAD-fluoromethyl ketone, partially blocked cell death induced by Survivin-T34A (Fig. 5*A*). Immunoblot analysis revealed fragmentation of PARP within 8 h after induction of Survivin-T34A, although cleavage of caspase-3 and -9 was barely detectable up through 48 h (Fig. 5*B*). These results suggested that caspase-independent pathways contribute to cell death induced by Survivin-T34A in t(17;19)$^+$ ALL cells.

The association of Survivin targeting both preceding and independent of caspase activation suggested to us a potential role for AIF, given its capacity to mediate DNA fragmentation

Downloaded from www.jbc.org at HIROSHIMA UNIVERSITY, on May 10, 2010

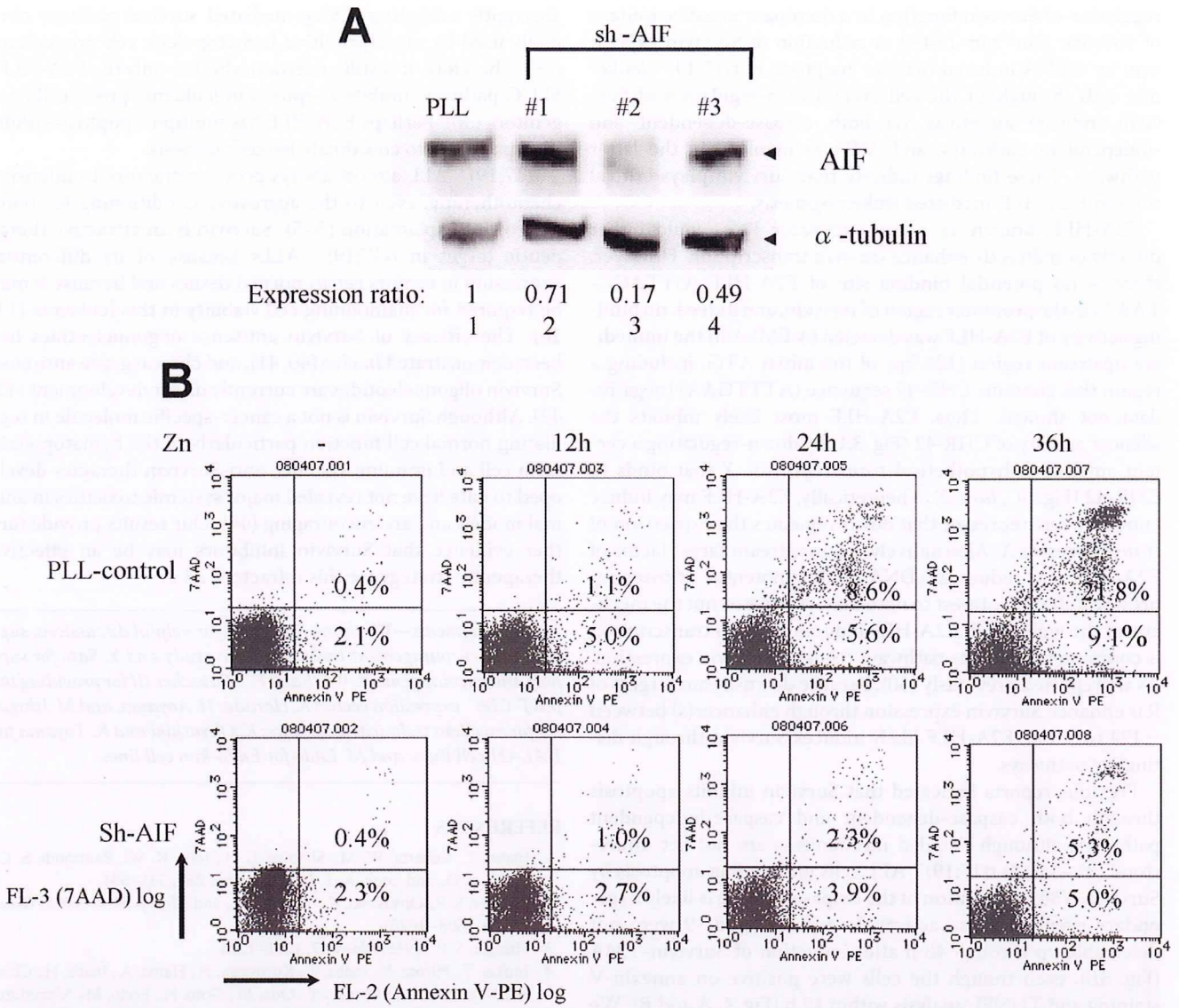

FIGURE 7. **Inhibition of Survivin-T34A-induced apoptosis by knockdown of AIF.** *A*, immunoblot analysis using AIF (*upper panel*) or α-tubulin (*lower panel*) antibodies. UOC-B1/Survivin(dn) cells were infected with lentivirus expressing the shRNA indicated *above* each panel, and GFP-positive cells were sorted. Ratios of intensity are shown *below*. *B*, UOC-B1/Survivin(dn) cells were infected with lentivirus expressing control-shRNA (*PLL*, *upper*) or AIF-shRNA2 (*lower*), cultured with 100 μM zinc for the indicated length of time, and stained with annexin-V-phycoerythrin (*PE*) (*abscissa*) and 7-AAD (*ordinate*). The data show the ratio of annexin-V-phycoerythrin- and 7-AAD-positive cells in the GFP-positive fraction as determined by flow cytometric analysis. *Numbers* indicate the percentage of apoptotic cells.

and cytochrome *c* release in a caspase-independent fashion (28, 29). We analyzed the nuclear translocation of AIF after induction of Survivin-T34A in t(17;19)$^+$ ALL cells. In the UOC-B1/Survivin(dn) cells without induction of Survivin-T34A, AIF signals were found in the cytoplasm in ~75% of the total cell population (Fig. 6*A*), consistent with a previous report showing the presence of AIF in mitochondria (27). By contrast, expression of Survivin-T34A for 12 h induced nuclear translocation of AIF signals in more than 90% of cells (Fig. 6*B*). Nuclear translocation of AIF was induced in only a small percentage (~ 4%) of the control UOC-B1/pMT cells treated with zinc (Fig. 6*D*).

To test the role of AIF in cell death induced by Survivin-T34A in t(17;19)$^+$ ALL cells, we down-regulated AIF expression by lentivirally expressed AIF-shRNA. The AIF protein expression level in UOC-B1/Survivin(dn) cells was significantly reduced by AIF-shRNA2 compared with that in cells infected with control PLL-shRNA sorted by expression of GFP (Fig. 7*A*). The number of cells undergoing cell death by induction of Survivin-T34A was monitored by annexin-V and 7-AAD staining in GFP-positive cells. Cells treated with AIF-shRNA2 were significantly resistant to cell death compared with those treated with control PLL-shRNA (Fig. 7*B*), suggesting that AIF plays critical roles in Survivin-mediated cell death of t(17;19)$^+$ ALL cells.

DISCUSSION

We previously demonstrated that E2A-HLF contributes to leukemogenesis of t(17;19)-positive ALL through inhibition of apoptosis (6). Here, we demonstrate that E2A-HLF induces Survivin expression through transcriptional regulation. Down-

Downloaded from www.jbc.org at HIROSHIMA UNIVERSITY, on May 10, 2010

regulation of Survivin function by a dominant negative mutant of Survivin (Survivin-T34A) or reduction of Survivin expression by shRNA induced massive apoptosis in t(17;19)$^+$ leukemia cells throughout the cell cycle. Down-regulation of Survivin induced apoptosis via both caspase-dependent and -independent pathways, and AIF was involved in the latter pathways. These findings indicate that Survivin plays critical roles in E2A-HLF-mediated leukemogenesis.

E2A-HLF, known as a *trans*-activator (24), could either directly or indirectly enhance *survivin* transcription. However, there is no potential binding site of E2A-HLF (GTTACGTAAT) in the promoter region of *survivin*, and indeed, no binding activity of E2A-HLF was detected by EMSA in the immediate upstream region (124 bp) of the initial ATG, including a region that contains CHR-42 sequence (ATTTGAA) (negative data not shown). Thus, E2A-HLF most likely inhibits the silencer activity of CHR-42 (Fig. 3*A*) by down-regulating a certain amount of hypothetical *trans*-repressor *X* that binds to CHR-42 (Fig. 3*C*, *lane 2*). Theoretically, E2A-HLF may induce another *trans*-repressor that down-regulates the expression of *trans*-repressor *X*. Alternatively, a downstream target factor of E2A-HLF may reduce the DNA binding potential of *trans*-repressor *X*. It is of interest to note that whether or not the mechanism through which E2A-HLF induces *survivin* transcription is common to that, Ras pathways regulate Survivin expression. As we reported previously (30), because downstream targets of Ras enhance Survivin expression through enhancer(s) between −124 to −190, E2A-HLF likely induces Survivin through distinctive pathways.

Previous reports indicated that Survivin inhibits apoptosis through both caspase-dependent and caspase-independent pathways, although detailed mechanisms are not yet understood (31–34). In t(17;19)$^+$ ALL cells undergoing apoptosis by Survivin-T34A, activation of the caspase cascade is likely a secondary event, because activated caspase-3 and -9 were not detectable up through 48 h after induction of Survivin-T34A (Fig. 5*B*), even though the cells were positive on annexin-V staining and TUNEL analysis within 12 h (Fig. 4, *A* and *B*). We observed rapid PARP activation within 8 h that is required for translocation of AIF to the nucleus from mitochondria, followed by morphological changes such as cell shrinkage and chromatin condensation (27, 35). Moreover, knockdown of AIF in UOC-B1/Survivin(dn) cells protected cells from apoptosis induced by Survivin-T34A (Fig. 7*B*). Therefore, reversal of AIF translocation by Survivin, which is induced by E2A-HLF throughout the cell cycle, appears to be the key mechanism in the protection of t(17;19)$^+$ leukemia cells from apoptosis.

In earlier studies, we identified *SLUG* as a target gene of E2A-HLF (36). SLUG is a transcription factor closely related to Ces-1, a cell death regulator in *Caenorhabditis elegans* (36, 37). Importantly, *ces-1* is a downstream target gene of *ces-2*, which is closely related to E2A-HLF (6, 38). The apparent convergence of cell death pathways, including CES-2/CES-1 in the worm and E2A-HLF/SLUG in human pro-B leukemia (6, 36), suggests that SLUG may have an important regulatory role in the survival of lymphoid cells. However, the lack of expression of Slug by normal pro-B cells suggests that E2A-HLF acts not by invoking a normal survival pathway in B lymphocytes but rather by aberrantly activating a Slug-mediated survival pathway normally used by more primitive hematopoietic cell progenitors (39). Therefore, it is still uncertain whether only the E2A-HLF/SLUG pathway inhibits apoptosis in leukemia pro-B cell progenitors (36). Perhaps E2A-HLF has multiple apoptosis-inhibiting pathways to coordinate leukemogenesis.

t(17;19)$^+$ ALL almost always proves refractory to intensive chemotherapy, even to the aggressive conditioning for bone marrow transplantation (3–5). Survivin is an attractive therapeutic target in t(17;19)$^+$ ALLs because of its differential expression in tumors *versus* normal tissues and because it may be required for maintaining cell viability in this leukemia (14, 16). The efficacy of Survivin antisense oligonucleotides has been demonstrated *in vivo* (40, 41), and clinical grade antisense Survivin oligonucleotides are currently under development (42, 43). Although Survivin is not a cancer-specific molecule in regulating normal cell function particularly in the hematopoietic stem cell and immune systems, anti-Survivin therapies developed to date have not revealed major systemic toxicities in animal models and are encouraging (44). Our results provide further evidence that Survivin inhibitors may be an effective therapeutic strategy for this refractory ALL.

Acknowledgments—We thank M. Eguchi for helpful discussions, support, and encouragement throughout this study and Y. Sato for support and encouragement. We thank F. J. Rauscher III for providing the pMT-CB6$^+$ expression vector; K. Harada, H. Aoyama, and M. Ishiguchi for excellent technical assistance; K. Ohyashiki and K. Toyama for HAL-O1 cell lines; and M. Endo for Endo-kun cell lines.

REFERENCES

1. Inaba, T., Roberts, W. M., Shapiro, L. H., Jolly, K. W., Raimondi, S. C., Smith, S. D., and Look, A. T. (1992) *Science* **257,** 531–534
2. Hunger, S. P., Ohyashiki, K., Toyama, K., and Cleary, M. L. (1992) *Genes Dev.* **6,** 1608–1620
3. Hunger, S. P. (1996) *Blood* **87,** 1211–1224
4. Inukai, T., Hirose, K., Inaba, T., Kurosawa, H., Hama, A., Inada, H., Chin, M., Nagatoshi, Y., Ohtsuka, Y., Oda, M., Goto, H., Endo, M., Morimoto, A., Imaizumi, M., Kawamura, N., Miyajima, Y., Ohtake, M., Miyaji, R., Saito, M., Tawas, A., Yanai, F., Goi, K., Nakazawa, S., and Sugita, K. (2007) *Leukemia* **21,** 288–296
5. Matsunaga, T., Inaba, T., Matsui, H., Okuya, M., Miyajima, A., Inukai, T., Funabiki, T., Endo, M., Look, A. T., and Kurosawa, H. (2004) *Blood* **103,** 3185–3191
6. Inaba, T., Inukai, T., Yoshihara, T., Seyshab, H., Ashmun, R. A., Canman, C. E., Laken, S. J., Kastan, M. B., and Look, A. T. (1996) *Nature* **382,** 541–544
7. Inukai, T., Inaba, T., Okushima, S., and Look, A. T. (1998) *Mol. Cell. Biol.* **18,** 6035–6043
8. Kinoshita, T., Yokota, T., Arai, K., and Miyajima, A. (1995) *EMBO J.* **14,** 266–275
9. Kuribara, R., Kinoshita, T., Miyajima, A., Shinjyo, T., Yoshihara, T., Inukai, T., Ozawa, K., Look, A. T., and Inaba, T. (1999) *Mol. Cell. Biol.* **19,** 2754–2762
10. Ikushima, S., Inukai, T., Inaba, T., Nimer, S. D., Cleveland, J. L., and Look, A. T. (1997) *Proc. Natl. Acad. Sci. U.S.A.* **94,** 2609–2614
11. Ambrosini, G., Adida, C., and Altieri, D. C. (1997) *Nat. Med.* **3,** 917–921
12. Sommer, K. W., Stumberger, C. J., Schmidt, G. E., Sasgary, S., and Cerni, C. (2003) *Oncogene* **22,** 4266–4280
13. Tamm, I., Wang, Y., Sausville, E., Scudiero, D. A., Vigne, N., Oltersdorf, T., and Reed, J. C. (1998) *Cancer Res.* **58,** 5315–5320
14. Li, F. (2003) *J. Cell. Physiol.* **197,** 8–29

Downloaded from www.jbc.org at HIROSHIMA UNIVERSITY, on May 10, 2010

15. Li, F., and Ling, X. (2006) *J. Cell. Physiol.* **208,** 476–486
16. Altieri, D. C. (2003) *Nat. Rev. Cancer* **3,** 46–54
17. Li, F., Ambrosini, G., Chu, E. Y., Plescia, J., Tognin, S., Marchisio, P. C., and Altieri, D. C. (1998) *Nature* **396,** 580–584
18. Li, F., and Altieri, D. C. (1999) *Biochem. J.* **344,** 305–311
19. Kurosawa, H., Goi, K., Inukai, T., Inaba, T., Chang, K. S., Shinjyo, T., Rake straw, K. M., Naeve, C. W., and Look, A. T. (1999) *Blood* **93,** 321–332
20. Kikuchi, J., Furukawa, Y., Iwase, S., Terui, Y., Nakamura, M., Kitagawa, S., Kitagawa, M., Komatsu, N., and Miura, Y. (1997) *Blood* **89,** 3980–3990
21. Rubinson, D. A., Dillon, C. P., Kwiatkowski, A. V., Sievers, C., Yang, L., Kopinja, J., Rooney, D. L., Zhang, M., Ihrig, M. M., McManus, M. T., Gertler, F. B., Scott, M. L., and Van Parijs, L. (2003) *Nat. Genet.* **33,** 401–406
22. Kikuchi, J., Shimizu, R., Wada, T., Ando, H., Nakamura, M., Ozawa, K., and Furukawa, Y. (2007) *Stem Cells* **25,** 2439–2447
23. Gu, C. M., Zhu, Y. K., Ma, Y. H., Zhang, M., Liao, B., Wu, H. Y., and Lin, H. L. (2006) *Neoplasm* **53,** 206–212
24. Inaba, T., Shapiro, L. H., Funabiki, T., Sinclair, A. E., Jones, B. G., Ashmun, R. A., and Look, A. T. (1994) *Mol. Cell. Biol.* **14,** 3403–3413
25. Kobayashi, K., Hatano, M., Otaki, M., Ogasawara, T., and Tokuhisa, T. (1999) *Proc. Natl. Acad. Sci. U.S.A.* **96,** 1457–1462
26. Deleted in proof
27. Moubarak, R. S., Yuste, V. J., Artus, C., Bouharrour, A., Greer, P. A., Menissier-de Murcia, J., and Susin, S. A. (2007) *Mol. Cell. Biol.* **27,** 4844–4862
28. Susin, S. A., Lorenzo, H. K., Zamzami, N., Marzo, I., Snow, B. E., Brothers, G. M., Mangion, J., Jacotot, E., Costantini, P., Loeffler, M., Larochette, N., Goodlett, D. R., Aebersold, R., Siderovski, D. P., Penninger, J. M., and Kroemer, G. (1999) *Nature* **397,** 441–446
29. Modjtahedi, N., Giordanetto, F., Madeo, F., and Kroemer, G. (2006) *Trends Cell Biol.* **16,** 264–272
30. Shinjyo, T., Kurosawa, H., Miyagi, J., Ohama, K., Masuda, M., Nagasaki, A., Matsui, H., Inaba, T., Furukawa, Y., and Takasu, N. (2008) *Tohoku J. Exp. Med.* **216,** 25–34
31. Carter, B. Z., Kornblau, S. M., Tsao, T., Wang, R. Y., Schober, W. D., Milella, M., Sung, H. G., Reed, J. C., and Andreeff, M. (2003) *Blood* **102,** 4179–4186
32. Liu, T., Brouha, B., and Grossman, D. (2004) *Oncogene* **23,** 39–48
33. Liu, T., Biddle, D., Hanks, A. N., Brouha, B., Yan, H., Lee, R. M., Leachman, S. A., and Grossman, D. (2006) *J. Invest. Dermatol.* **126,** 2247–2256
34. Croci, D. O., Cogno, I. S., Vittar, N. B., Salvatierra, E., Trajtenberg, F., Podhajcer, O. L., Osinaga, E., Rabinovich, G. A., and Rivarola, V. A. (2008) *J. Cell. Biochem.* **105,** 381–390
35. Yu, S. W., Wang, H., Poitras, M. F., Coombs, C., Bowers, W. J., Federoff, H. J., Poirier, G. G., Dawson, T. M., and Dawson, V. L. (2002) *Science* **297,** 259–263
36. Inukai, T., Inoue, A., Kurosawa, H., Goi, K., Shinjyo, T., Ozawa, K., Mao, M., Inaba, T., and Look, A. T. (1999) *Mol. Cell* **4,** 343–352
37. Metzstein, M. M., and Horvitz, H. R. (1999) *Mol. Cell* **4,** 309–319
38. Metzstein, M. M., Hengartner, M. O., Tsung, N., Ellis, R. E., and Horvitz, H. R. (1996) *Nature* **382,** 545–547
39. Inoue, A., Seidel, M. G., Wu, W., Kamizono, S., Ferrando, A. A., Bronson, R. T., Iwasaki, H., Akashi, K., Morimoto, A., Hitzler, J. K., Pestina, T. I., Jackson, C. W., Tanaka, R., Chong, M. J., McKinnon, P. J., Inukai, T., Grosveld, G. C., and Look, A. T. (2002) *Cancer Cell* **2,** 279–288
40. Tu, S. P., Jiang, X. H., Lin, M. C., Cui, J. T., Yang, Y., Lum, C. T., Zou, B., Zhu, Y. B., Jiang, S. H., Wong, W. M., Chan, A. O., Yuen, M. F., Lam, S. K., Kung, H. F., and Wong, B. C. (2003) *Cancer Res.* **63,** 7724–7732
41. Kanwar, J. R., Shen, W. P., Kanwar, R. K., Berg, R. W., and Krissansen, G. W. (2001) *J. Natl. Cancer Inst.* **93,** 1541–1552
42. Schimmer, A. D. (2004) *Cancer Res.* **64,** 7183–7190
43. Altieri, D. C. (2008) *Nat. Rev. Cancer* **8,** 61–70
44. Fukuda, S., and Pelus, L. M. (2006) *Mol. Cancer Ther.* **5,** 1087–1098

Downloaded from www.jbc.org at HIROSHIMA UNIVERSITY, on May 10, 2010